The Impact of Reduced Kidney Mass on Adipose Tissue Metabolism and Whole-body Glucose Homeostasis in Mice

---

Dissertation

zur

Erlangung der naturwissenschaftlichen Doktorwürde
(Dr. sc. nat.)

vorgelegt der

Mathematisch-naturwissenschaftlichen Fakultät

der

Universität Zürich

von

Siew Hung Chin

aus

Malaysia

Promotionskomitee

Prof. Dr. François Verrey (Vorsitz)

Prof. Dr. Daniel Konrad (Leitung der Dissertation)

Prof. Dr. Matthias R. Baumgartner

Prof. Dr. Wolfgang Langhans

Zürich, 2014

Table of Contents

Acknowledgement

First of all, I am heartily thankful to my supervisor Prof. Dr. med. Daniel Konrad for his valuable guidance, encouragement and advice from the initial to the end of this doctoral dissertation enabling me to develop an understanding of the subject. Especially, I would like to express my profound gratitude to Dr. Stephan Wüest and Dr. Flurin Item for providing timely support, caring and favourable environment in the group to achieve this research project.

I am grateful to my research advisory committee members, Prof. Dr. François Verrey, Prof. Dr. Matthias R. Baumgartner, Prof. Dr. Wolfgang Langhans for spending their time and giving constructive suggestions during meetings.

I am thankful to my lab colleagues Michael Wiedemann and Fabrizio Lucchini for helpful discussion and creating a pleasant atmosphere in the laboratory.

It is enjoyable to have lab fellows from the C Lab, Dr. Richard Züllig, Dr. Markus Niessen, Maren Dietrich, Heidi Seiler, Diri Schmid, Claudia Ghirlanda-Keller, Cornelia Zwimpfer, Michèle Rothfuchs, Amir Mizbani, Artur Galimov, Tatiane Gorsko, Angelika Hartung, Katarina Turcekova, all have extended their support in a special way. Special massive thanks to all of you for scholarly interactions and great company during coffee time in the past 3.5 years.

Lastly, I offer my sincere regards to my family that encouraged me in any respect during my restless travelling in Europe and my studies in Zurich.

Summary

Reduced kidney mass by uninephrectomy may result in multiple metabolic derangements, including insulin resistance (IR). In this regard, using the 'gold standard' hyperinsulinaemic-euglycaemic clamp technique, DeFronzo et al. found evidence of reduced insulin responsiveness in peripheral tissues of chronic kidney disease (CKD) patients, most likely in skeletal muscle tissues. However, the underlying mechanisms still remain unclear. The principal goal of the present project was to determine the impact of reduced kidney mass on glucose metabolism in lean and obese mice. To this end, male C57BL6/J mice underwent uninephrectomy (UniNx) or sham operation at 7 weeks of age. After surgery, animals were fed either chow (standard) or high fat diet (HFD). Glucose homeostasis was assessed 2, 8 and 20 weeks after surgery. No significant differences were observed in glucose tolerance between sham-operated and UniNx mice. However, skeletal muscle insulin resistance as assessed by hyperinsulinaemic-euglycaemic clamp was significantly deteriorated in HFD-fed UniNx mice, whereas insulin-stimulated glucose uptake into isolated skeletal muscle was similar between HFD-fed sham-operated and UniNx mice. Importantly, capillary density was significantly reduced in skeletal muscle of HFD-fed UniNx mice. In contrast, hepatic insulin sensitivity was improved and HFD-induced adipose tissue inflammation was reduced in UniNx mice. Moreover, expression of hypoxia inducible factor 1-alpha (HIF1α) was reduced in adipose tissue of HFD-fed UniNx mice. However, treatment with the angiotensin II type I receptor blocker i.e. telmisartan improved glucose tolerance and hepatic insulin sensitivity only in HFD-fed sham-operated mice but not HFD-fed UniNx mice. In conclusion, UniNx protects from obesity-induced adipose tissue inflammation and hepatic insulin resistance potentially via a reduction in HIF1α expression. In contrast, UniNx reduces muscle capillary density, and thus deteriorates HFD-induced skeletal muscle glucose disposal *in vivo*.

Zusammenfassung

Eine reduzierte Nierenmasse infolge Uninephrektomie kann zu metabolischen Komplikationen wie zum Beispiel einer Insulinresistenz führen. Dementsprechend fanden DeFronzo und Kollegen in hyperinsulinämen-euglykämen Clamp Studien in Patienten mit chronischer Nierenkrankheit eine verminderte Insulinsensitivität in peripheren Geweben, wobei vermutlich vor allem der Skelettmuskel von einer Insulinresistenz betroffen war. Der dahinterliegende Mechanismus ist jedoch nicht vollumfänglich bekannt. Ziel dieses Projektes war es, den Einfluss einer reduzierten Nierenmasse auf den Zuckerstoffwechsel in schlanken und übergewichtigen Mäusen zu untersuchen. Dazu wurden männliche C57BL6/J Mäuse im Alter von 7 Wochen einer Uninephrektomie (UniNx) oder einer Scheinoperation unterzogen. Nach der Operation erhielten die Mäuse entweder eine Standardnahrung oder eine fettangereicherte Diät und der Zuckerstoffwechsel wurde 2, 8 und 20 Wochen postoperativ untersucht. Dabei ergab sich kein Unterschied in der Glukosetoleranz zwischen scheinoperierten und uninephrektomierten Mäusen. Hingegen fand sich während hyperinsulinämen-euglykämen Clamp Studien in übergewichtigen Mäusen eine signifikant verschlechterte Insulinsensitivität in der Skelettmuskulatur in UniNx Mäusen, während die insulinstimulierte Glukoseaufnahme in die isolierte Skelettmuskulatur nicht beeinträchtigt war. Interessanterweise war die Kapillardichte in Skelettmuskeln von übergewichtigen UniNx Mäusen signifikant reduziert. Im Gegensatz zur Insulinsensitivität im Skelettmuskel fand sich eine verbesserte Leberinsulinsensitivität sowie eine reduzierte Entzündung im Fettgewebe in UniNx Mäusen. Ebenfalls war die Expression von HIF1α tiefer im Fettgewebe uninephrektomierter Mäuse. Eine Behandlung der Mäuse mit dem Angiotensin II Typ I Rezeptor Blocker Telmisartan verbesserte die Glukosetoleranz und die Leberinsulinsensitivität nur in übergewichtigen scheinoperierten, nicht aber in UniNx Mäusen. Zusammenfassend schützt eine Uninephrektomie von einer übergewichts-bedingten Entzündung des Fettgewebes sowie einer Leberinsulinresistenz, was vermutlich die Folge einer reduzierten Expression von HIF1α ist. Im Gegensatz dazu

vermindert die Entfernung einer Niere die Kapillardichte im Skelettmuskel, was zu einer verschlechterten Glukoseaufnahme *in vivo* führt.

Abbreviations

Akt/PKB	protein kinase B
AS160	akt substrate of 160kDa
BSA	bovine serum albumin
BMI	body mass index
cDNA	complementary deoxyribonucleic acid
CKD	chronic kidney disease
EGP	endogenous glucose production
ESRD	end stage renal disease
FFAs	free fatty acids
GLUT	glucose transporter
GTT	glucose tolerance test
GFR	glomerular filtration rate
GIR	glucose infusion rate
HFD	high fat diet
HIF1α	hypoxia inducible factor 1-alpha
IS GDR	insulin-stimulated glucose disposal rate
IRS	insulin receptor substrate
IL-6	interleukin-6
ip	intraperitoneal
ITT	insulin tolerance test
JNK	jun N-terminal kinase
MAPK	mitogen-activated protein kinase
mRNA	messenger ribonucleic acid
PI3K	phosphatidylinositide-3-kinase
PIP3	phosphatidylinositol-3,4,5-triphosphate
PKC	protein kinase C

RAS	renin-angiotensin-system
rt-PCR	real-time polymerase chain reaction
T2DM	type 2 diabetes mellitus
TG	triacylglycerol
TNFα	tumour necrosis factor-alpha
UniNx	uninephrectomy
WAT	white adipose tissue

1 Introduction

1.1 Obesity

1.1.1 Prevalence of obesity

Overweight, defined as a body mass index (BMI, defined as the individual's body mass divided by the square of height) [1] equal to or more than 25 kg/m^2, and obesity, defined as BMI greater than 30 kg/m^2, are characterized by excessive fat accumulation resulting from an imbalance between energy intake and energy expenditure. Worldwide, it is estimated that there are more than 300 million obese adults [1]. According to the recent epidemiological reports, the prevalence of obesity is increasing in most societies, even among young adults and children [2, 3]. Furthermore, there is evidence that obesity is a major risk factor for the development of various diseases, the most devastating of which may be type 2 diabetes mellitus (T2DM) [4]. Concurrent with the rising prevalence of obesity is an epidemic of chronic kidney disease with an estimated 11% of the United States population currently affected [5]. It is estimated that 60% of all end stage renal disease (ESRD) patients who receive a kidney transplant are either overweight or obese at the time of transplantation [6]. Data from studies in the United States have suggested that, unabated, increasing demand for live-donor kidneys has encouraged the use of obese donors [7]. Obesity is affected by a complex interaction. Although the growing obesity epidemic reflects profound changes in diet and physical activity (sedentary life-style) over recent decades, genetic factors are important in determining individual's susceptibility to weight gain and adverse health consequences of obesity [1]. Because of the increased health risks associated with obesity, the obesity epidemic places a large financial burden on the economy. It has therefore emerged as one of the most pressing global issues that we will face during the next several decades in the modern society.

1.1.2 Inflammation

In obesity, adipose tissue expansion is associated with local infiltration of different types of inflammatory cells, especially macrophages [8]. These macrophages are predominantly M1 polarized (CD11c+) and are characterized by increased release of proinflammatory cytokines, such as tumour necrosis factor (TNF)-α, interleukin (IL)-6, and IL-1 among others [9, 10]. In contrast, adipose tissue of lean mice contains mainly alternatively activated, anti-inflammatory M2 macrophages [11]. The overproduction of proinflammatory cytokines contributes to the induction of insulin resistance (defined as the diminished ability of cells to respond to insulin, i.e. resulting in reduced glucose uptake into muscle and adipose tissue and decreased suppression of hepatic glucose output) both locally and systemically, i.e. in skeletal muscle and liver [12]. For instance, proinflammatory cytokines such as IL-6 reduce insulin-stimulated glucose uptake into adipocytes and skeletal muscle through its ability to inhibit tyrosine phosphorylation of IRS-1 [13, 14]. TNF-α affects the stability of lipid droplets in adipocytes by decreasing perilipin expression [15]. In addition, TNF-α was described to induce excess adipose lipolysis, which could drive fatty acid re-esterification and ectopic lipid accumulation, promoting impaired insulin signal transduction [16].

Adipose tissue hypoxia may contribute to adipose tissue inflammation and develops as a consequence of limited vascular supply of expanding adipose tissue [17]. Hypoxia results in increased expression of hypoxia inducible factor 1-alpha (HIF1α) [18]. Importantly, selective inhibition of HIF1α was previously reported to reduce adipose tissue inflammation in obese mice [19]. Conversely, overexpression of HIF1α induced adipose tissue inflammation [20].

Expression of pro-inflammatory cytokines may differ between fat depots. Especially, intra-abdominal fat depots (e.g. omental and mesenteric white adipose tissue) show a higher degree of cytokine expression [21, 22]. The increased release of pro-inflammatory cytokines (and free fatty acids) from these depots directly drain into the portal vein which contributes to the development of hepatic insulin resistance and steatosis

[23]. In conclusion, adipose tissue inflammation is a hallmark of obesity and plays a role in the development of obesity-associated metabolic dys-regulation such as insulin resistance.

1.1.3 Ectopic lipid accumulation

In healthy subjects, white adipose tissue (WAT) is able to expand to store any surplus of calories as triglycerides. In obesity, however, the storage capacity of WAT may be limited [24]. Especially, expandability of subcutaneous adipose tissue is constricted resulting in increased lipid accumulation in intra-abdominal fat depots as well as in liver, skeletal muscle and heart [25, 26]. This ectopic fat deposition including intramyocellular triglyceride accumulation and production of toxic lipid metabolites may exert deleterious effects, such as impaired insulin signalling, in different tissues [27, 28]. Interestingly, ectopic lipid accumulation is also a characteristic feature of lipodystrophy, a disorder characterized by selective loss of body fat [29]. Consequently, adipose tissues cannot sufficiently buffer postprandial influx of fatty acids, resulting in increased fat storage in liver, skeletal muscle and other peripheral tissues and subsequently cause impairment of insulin signalling [25]. Importantly to the present thesis, studies in rodents suggest that reduced kidney mass due to uninephretomy may result in a state of acquired lipodystrophy leading to ectopic lipid deposition.

1.1.4 Renin-angiotensin-system activation

The renin-angiotensin-system (RAS) regulates blood pressure and water (fluid) balance [30, 31]. Moreover, there is growing evidence that activation of the RAS may play a role in obesity-associated insulin resistance [32]. Over the last decades, components of the RAS such as renin, angiotensinogen (AGT), angiotensin II (ATII) were thought to be exclusively produced by liver, kidney, and vasculature. However, current studies have prevailed that local RAS exists in numerous organs such as pancreas, heart, brain, and white adipose tissue (WAT) [33, 34]. Particularly, WAT synthesizes and secretes the major components of the RAS [35]. In obesity, the adipose RAS is activated. Several lines of

evidence have shown that adipose RAS overactivation may induce insulin resistance via increasing adipose tissue inflammation [32, 36]. Moreover, recent studies have suggested that inactivation of the RAS in animal models improves insulin sensitivity and protects from diet-induced obesity and insulin resistance [37-39]. In particular, telmisartan, which is an angiotensin II type 1 receptor blocker, was previously reported to improve obesity-induced adipose tissue inflammation [40, 41]. These findings highlight the potential role for activation of the adipose RAS in the development of obesity-associated insulin resistance. Reduced renal function e.g. in the context of renal inflammation and reduced glomerular infiltration leads to increased activation of the RAS [42]. Moreover, it has been reported that chronic renal impairment was associated with fat redistribution and increased triacyglycerol levels and, thus, may contribute to the development of insulin resistance [43, 44]. These findings therefore support the notion that chronic renal impairment may lead to adipose tissue dysfunction and insulin resistance via activation of the RAS.

1.2 Insulin resistance

1.2.1 Definition of insulin resistance

Insulin resistance is a prerequisite for the development of T2DM and may be partly responsible for the increased risk of CKD [45, 46]. Clinically, insulin resistance can be broadly defined as a blunt biological response to normal levels of circulating insulin, resulting in compensatory hyperinsulinaemia [47]. Insulin resistance can be determined by the homeostatic model assessment HOMA–IR (calculated from fasting plasma glucose and fasting plasma insulin levels) or more sophisticatedly by hyperinsulinaemic-euglycaemic clamp studies (gold standard for the assessment of insulin resistance) [48, 49].

Insulin’s action in various tissues is complex and it regulates many biological processes. For instance, insulin increases glucose uptake in skeletal muscle and adipose tissue. In the liver, it suppresses hepatic glucose production [50, 51]. Additionally, it also stimulates lipogenesis and triglyceride secretion, regulates many other processes including bile acid metabolism, growth and differentiation [52-54]. Clinical definition of insulin

resistance implies that all of these processes become resistant, though this is unlikely to be true. Indeed, some pathway remains sensitive to insulin, while other pathways become resistant, particularly glucose uptake into skeletal muscle and inhibition of hepatic glucose production [55-57]. Therefore, insulin resistance may appear in one of the target organs even in the absence of systemic impaired glucose homeostasis.

1.2.2 Insulin signalling pathway

Insulin is synthesized and secreted by pancreatic β-cells dependent on blood glucose concentration. Upon binding of insulin, the insulin receptor is auto-phosphorylated leading to activation of its endogenous tyrosine kinase and subsequently phosphorylating tyrosine residues on insulin receptor substrate (IRS) [58]. Two major signalling pathways are activated in response to insulin: the phosphoinositide 3-kinase (PI3K) and the mitogen-activated protein (MAP) kinase pathway. Tyrosine phosphorylation of insulin receptor substrates (IRS) activates phosphatidylinositide-3-kinase (PI3K), this providing a docking site for the p85 regulatory subunit and releasing the p110 catalytic subunit. PI3K triggers activation of the 3-phosphoinositide-dependent protein kinase 1 (PDK1) kinase and Akt kinase [50, 59]. The PI3K-Akt pathway is responsible for many of the downstream metabolic effects of insulin [60]. In skeletal muscle and adipose tissue, Akt kinase stimulates translocation of insulin-sensitive glucose transporter (GLUT4) to the plasma membrane and facilitates the glucose uptake [61]. In vascular endothelial cells, Akt kinase phosphorylates and activates endothelial nitric oxide synthase (eNOS) [62]. In parallel, tyrosine phosphorylation of the Shc protein activates the GTP exchange factor Sos [63]. This may result in inactivation of the MAP kinase pathway, involving Ras, MAP kinase and extracellular regulated kinase (ERK). The MAP kinase pathway mediates endothelin-1 (ET-1) production, leading to vasoconstriction, growth and mitogenesis effects on vascular smooth muscle cells, and among others (**Figure 1**) [64]. Insulin resistance may occur as a result of interference with the insulin signalling cascade at any level [65].

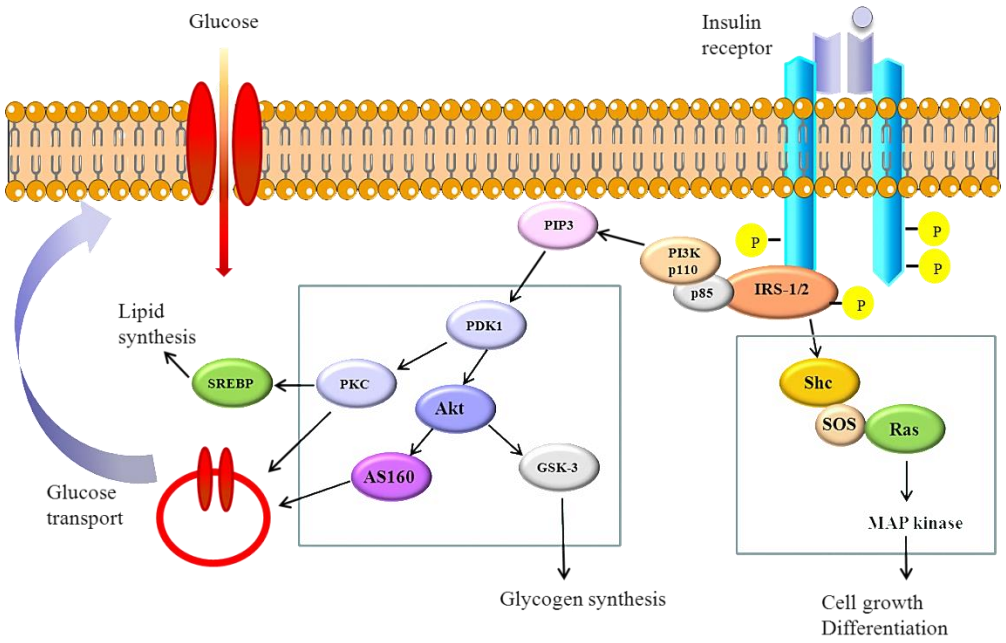

Figure 1. Signal transduction in insulin action. The insulin receptor is a tyrosine kinase that undergoes autophosphorylation and catalyses the phosphorylation of cellular proteins such as members of the IRS family, Shc. Upon tyrosine phosphorylation, these proteins interact with signalling molecules, resulting in a diverse series of signalling pathways, including activation of PI3K, ras and the MAP kinase cascade. These pathways act in a concerted fashion to coordinate the regulation of glucose, lipid and protein metabolism (modified from Taniguchi et al. 2006 [50], the illustration was created in part with Servier Medical Art, www.servier.com).

1.2.3 Metabolic effects of insulin resistance in adipose tissue and liver

Accumulation of triacyglycerol in adipose tissue, as in obesity, is associated with insulin resistance [66]. In contrast, as outlined above, deficiency of adipose tissue as in lipodystrophy is also associated with insulin resistance [67, 68]. As a result, there is an increased release of free fatty acids (and cytokines) and subsequently ectopic fat deposition. All these changes may impair insulin signalling in different tissues. Interestingly, both obesity and lipodystrophy are related to CKD [69]. Experimentally, reduced kidney mass as established by uninephrectomy in rats results in lipodystrophy and is accompanied by low-grade inflammation [44, 70].

Ectopic lipid accumulation in the liver is associated with hepatic steatosis as well as hepatic insulin resistance [71, 72]. Both conditions are also associated with chronic low-

grade inflammation in WAT [73, 74]. The portal theory claims that an excess flow of FFAs and pro-inflammatory cytokines arising from insulin-resistant visceral adipose tissue in obesity are rapidly translocated to the liver via portal circulation, where they reassembled into triglycerides, promoting the development of hepatic steatosis and induce insulin resistance [23].

1.2.4 Defects of insulin resistance and microcirculation in skeletal muscle

Skeletal muscle plays a major role in glucose metabolism, accounting for 80% of whole-body insulin stimulated glucose disposal [75]. It has been suggested that skeletal muscle lipid oversupply is associated with insulin resistance [76]. Skeletal muscle insulin resistance is the result of reduced IRS-1 activation of PI3K and, consequently, diminished GLUT4 translocation to the membrane surface [77]. In addition to facilitating the transport of glucose into muscle cells, insulin increases microvascular perfusion of the muscle and that accounts for approximately half of the insulin-mediated glucose uptake [78-80]. The increase in insulin-mediated microvascular recruitment is diminished in states of insulin resistance and, thus, reduced muscle tissue perfusion contributes to insulin resistance [81, 82]. Accordingly, insulin resistant subjects exhibit capillary rarefaction [79, 83, 84]. Underlying mechanisms leading to diminished insulin mediated blood flow remain unclear.

1.3 Type 2 diabetes mellitus

1.3.1 The development of type 2 diabetes mellitus

The incidence and prevalence of diabetes mellitus is increasing worldwide over the last decades [85]. Epidemiological data show that over three hundred million people were diagnosed with type 2 diabetes mellitus (T2DM) in 2010 and the prevalence will further rise at an alarming rate [86]. The nature of the inherited defect of diabetes is still unknown, but acquired metabolic abnormalities are closely linked to several factors, in particular obesity. Indeed, obesity is believed to account for 80% of the risk of developing T2DM [87,

88]. Obesity initially leads to the development of insulin resistance in adipose and other tissues. Consequently, insulin resistance is compensated by increased insulin secretion. However, the pancreatic beta cells eventually fail to produce sufficient amount of insulin to overcome insulin resistance, leading to hyperglycaemia and ultimately T2DM [89]. Chronic inflammation especially in adipose tissue appears to play a major role in disease development and progression [66]. As previously mentioned, released proinflammatory cytokines may induce insulin resistance and contribute to beta cell dysfunction. Accordingly, such inflammatory mediators appear to be markers to predict impaired glucose tolerance [90-92].

1.3.2 Diabetic nephropathy

T2DM is associated with increased morbidity and mortality due to complications occurring as a consequence of chronic hyperglycaemia and/or chronic hyperinsulinaemia [93]. Especially, eyes, kidneys, the nervous system, and peripheral arteries are often affected [94, 95]. Diabetic nephropathy is characterized by increasing microalbuminuria, decreasing glomerular filtration rate, hypertension and other diabetic-associated complications [96]. It is a progressive disease and may lead to end stage renal disease (ESRD) with the need for dialysis or kidney transplantation [97]. T2DM is the most common cause for acquired ESRD in Western society and, thus, the rapidly rising trend of T2DM prevalence is of major concern [98, 99].

Undoubtedly, T2DM is causing chronic kidney dysfunction. However, there is evidence that the opposite may be also true, i.e. that reduced kidney function/mass may facilitate the development of the metabolic syndrome as suggested for kidney donors [100]. Moreover, Ibrahim et al. reported on 154 living kidney donors developing T2DM after kidney donation [101]. In addition, uninephrectomy in rats was reported to impair glucose tolerance [43, 44]. However, the underlying mechanisms are poorly understood. Furthermore, such data are rather scarce and further investigation is needed.

1.4 Chronic kidney disease

1.4.1 The risk of chronic kidney disease

The kidneys play an important role in the maintenance of whole body homeostasis. Notably, the kidneys contribute to the regulation of fluid, electrolyte and acid-base balance, to the excretion of metabolic waste, and, most relevant to the discussion of this project, to glucose metabolism [102, 103]. The kidneys reabsorb around 180 g of glucose per day, thereby assisting to maintain normal fasting plasma glucose levels at ~5-6 mmol/l which ensures that sufficient energy is available especially for the brain during fasting periods [104]. However, when plasma glucose concentration exceeds 12 mmol/l which is the maximal reabsortive capacity of the two kidneys, glycosuria will occur [105]. CKD represents a progressive and irreversible decline in kidney function and is characterized by a glomerular filtration rate (GFR) of less than 60 ml/min per 1.73 m^2 for more than three months [106]. Decreased GFR is associated with obesity, diabetes, hypertension, and dyslipidaemia [107-109].

There is increasing evidence that obese patients are more susceptible to the development of CKD [110]. Studies demonstrate that subjects with severe obesity develop proteinuria with glomerular enlargement, mesangial expansion, podocyte hypertrophy, and glomerular sclerosis [111-113]. Virtually, all chronic kidney diseases are usually progressive and may lead to renal failure [106, 114]. Renal failure is a loss of renal function characterized by uraemia and retention of nitrogenous waste in the blood [106]. Around 30% of all diabetics develop evidence of nephropathy which may lead to ESRD and the latter is the leading cause for kidney transplantation in most countries [115]. It has resulted in a markedly increased demand for live kidney donors [97]. Conversely, it remains unclear whether CKD per se can induce T2DM and other components of the metabolic syndrome. However, there is evidence for mild fasting hyperglycaemia and abnormal glucose tolerance in nondiabetic patients with ESRD [116, 117]. In addition, live kidney donors may have impaired glucose homeostasis [101, 118]. Yet, available evidence is largely unrecognized.

1.4.2 Animal model of uninephrectomy and diet-induced obesity

Reduced kidney mass can experimentally be induced in rodents by uninephrectomy [119, 120]. This model closely resembles progressive renal disease in human and it shows a high degree of reproducibility [121]. Thus, uninephrectomy may be a preferred model of mimicking the clinical situation of kidney donation [122]. However, some rodent studies suggest that contralateral uninephrectomy and the resulting mild decreased kidney function was not enough to cause progression, and that, accelerants were essential [123, 124]. In the present study, diet-induced obesity was used as an accelerant of disease progression in mouse uninephrectomy model. It was previously reported that uninephrectomy in rats was associated with elevated expression of angiotensin type 1 receptor and insulin resistance [43]. In addition, uninephrectomy leads to adipose tissue redistribution with increased visceral adipose tissue mass known to be associated with the development of (hepatic) insulin resistance [44]. Thus, uninephrectomy may be a good model to study the impact of reduced kidney mass on glucose homeostasis and the development of insulin resistance.

1.4.3 Crosstalk of kidney disease with adipose tissue, liver, and skeletal muscle

Recent studies suggested that obesity, which is associated with adipose tissue dysfunction, contributes to the observed increase in the incidence of CKD [125, 126]. Accumulating data demonstrated that renal lipid accumulation and lipotoxicity in diet-induced obese mice may lead to kidney dysfunction [127, 128]. Conversely, experimental studies showed that CKD induced by uninephrectomy is associated with adipose tissue dysfunction, resulting in ectopic lipid stores in multiple organs [70]. In a model of uninephrectomised rats, Zhao et al. reported that uninephrectomy-associated lipodystrophy may lead to ectopic lipid redistribution in liver, skeletal muscle, kidney and many other tissues [44]. Additionally, the uninephrectomised rats developed glucose intolerance and hyperinsulinaemia [43]. Thus, these studies provide evidence for a crosstalk between the

injured kidney and distant organs, particularly adipose tissue, liver, and skeletal muscle (**Figure 2**). Previous reports have revealed that abnormalities in lipid and glucose metabolism in the kidney contribute to the development of dysfunction in other organs such as adipose tissue. It was hypothesized that such adipose tissue dysfunction then resulted in ectopic lipid redistribution [70]. In addition, ongoing crosstalk between kidney and adipose tissue may impact on the secretion pattern of adipocytokines and RAS components contributing to the development of systemic insulin resistance and inflammation [39, 129]. Moreover, the increased production and release of pro-inflammatory cytokines from (visceral) adipose tissue promote the development of hepatic insulin resistance and steatosis as suggested by the portal theory [23].

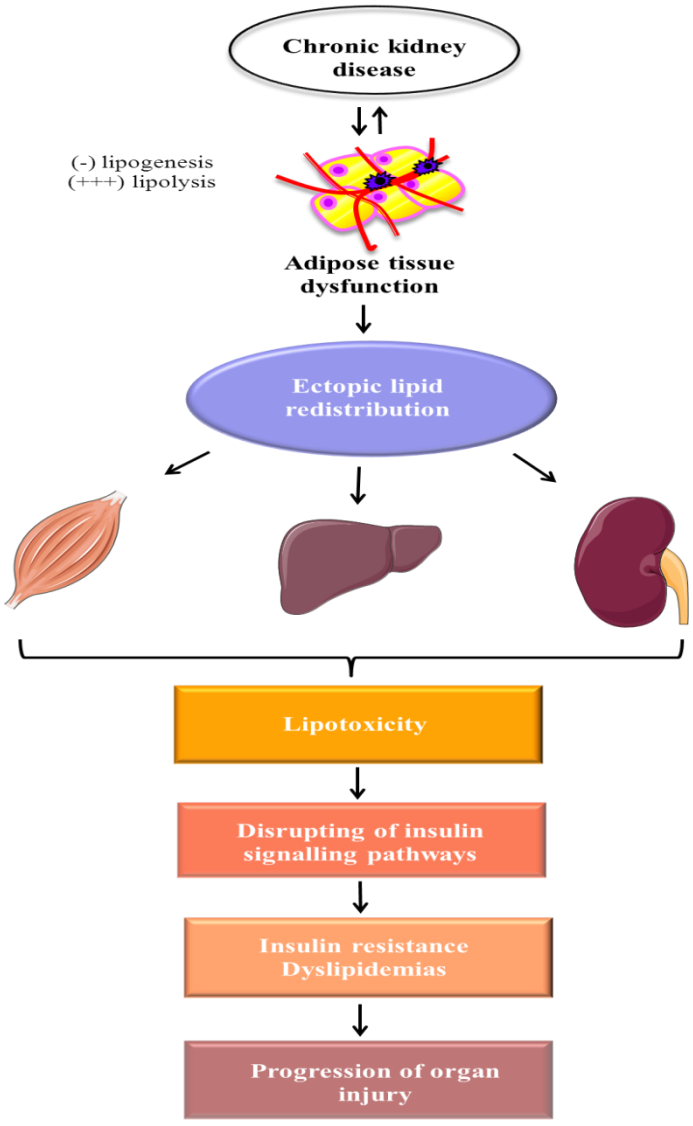

Figure 2 Dysfunctional crosstalk between kidney, adipose tissue, liver, and skeletal muscle. Chronic kidney disease induces adipose tissue dysfunction. Adipose tissue dysfunction with limited ability to store excess energy results in lipid deposition at nonadipose sites such as liver, skeletal muscle and kidney. Intracellular lipid accumulation might impair insulin signalling, leading to insulin resistance and dyslipidaemia, and eventually promote multiple organ injuries.

On the other hand, CKD as well as obesity may promote ectopic lipid accumulation resulting non-alcoholic fatty liver disease (NAFLD) [70, 130, 131]. NAFLD can exacerbate hepatic insulin resistance and subsequently further increase in whole-body insulin resistance [132]. Besides promoting ectopic lipid accumulation, CKD is associated with increased activation of the RAS, which was demonstrated to contribute to the development of hepatic fibrogenesis [133, 134]. Thus, CKD may propagate (obesity-associated) adipose tissue dysfunction as well as hepatic steatosis and insulin resistance.

Recent experimental and clinical evidence demonstrated evidence for a cross-talk between skeletal muscle and kidney in the pathogenesis of obesity-related renal disease. In patients with CKD, muscle atrophy is common and studies of animal models of CKD indicate that kidney dysfunction is associated with muscle atrophy through activation of angiotensin II (Ang II) [44, 135, 136]. The catabolic effect of Ang II is mediated by impaired insulin /IGF-1 intracellular signalling leading to protein degradation in muscle [137, 138]. Such phenomenon may be responsible, at least in part, for the observed reduction of muscle mass, as RAS is frequently activated in the progression of renal disease [139-141]. In addition, animal models of CKD reported an association between ectopic lipid accumulation and insulin resistance [43, 70]. As outlined above, accumulation of intramyocellular lipids inhibits insulin signalling by activating PKC-θ resulting in skeletal muscle insulin resistance [142, 143]. Importantly, DeFronzo et al. demonstrated that peripheral insulin-mediated glucose uptake was decreased in patients with ESRD [116]. However, cellular mechanisms linking CKD to skeletal muscle lipid accumulation and/or insulin resistance remain to be fully clarified.

Thus, kidney function may not only deteriorate in the progression of obesity but kidney dysfunction may also negatively impact on adipose function and (consequently) to total-body insulin sensitivity.

1.5 Aim of the study

Reduced kidney mass deteriorates insulin sensitivity. However, underlying mechanisms are poorly understood. In the present thesis, we hypothesize that reduced kidney mass impairs glucose metabolism and insulin sensitivity via activation of the RAS in adipocytes (**Figure 3**).

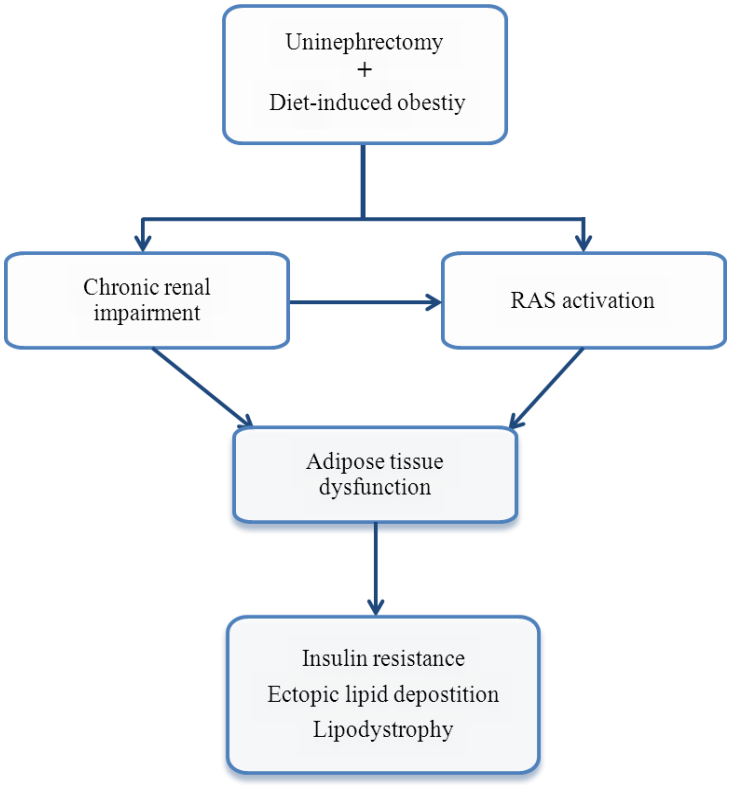

Figure 3 Schematic illustration of possible mechanisms leading to adipose tissue dysfunction, and subsequently to insulin resistance in individuals with reduced kidney mass. Reduced kidney mass may impair or alter adipose tissue function through two different mechanisms: 1) it may induce chronic renal impairment; 2) activation of the RAS

2 Materials and methods

2.1 Animals

Male C57BL/6J (C57BL/6JOlaHsd) mice were purchased from Harlan Netherlands (Harlan, Horst, the Netherlands). All mice were housed in a specific pathogen-free environment on a 12-hours-light-dark cycle (light on from 7 pm to 7 am) and fed *ad libitum* with regular chow diet (ProvimiKliba, Kaiseraugst, Switzerland) or high fat diet (HFD) (58 kcal% fat w/sucrose Surwit Diet, D12331, Research Diets). All protocols conformed to the Swiss animal protection laws and were approved by the Cantonal Veterinary Office in Zurich, Switzerland.

2.2 Diets

Table I lists the ingredients of the chow diet and high fat diet.

Table 1 Content of chow and high fat diet.

Ingredients	Chow diet	High-fat diet
Protein (kcal%)	31	16.4
Carbohydrate (kcal%)	57	25.5
Fat (kcal%)	12	58.0

2.3 Surgical procedure

Male C57BL/6J mice underwent uninephrectomy or sham operation at 7 weeks of age. Mice were anaesthetized with isoflurane (Abbott, Baar, Switzerland). Eye ointment (Vitamin A “Blanche”, Bausch & Lomb Swiss AG) was applied to both eyes. Mice were placed on a warming-pad and kept under an infrared heating lamp to stabilize body temperature during the whole surgical procedure. Left nephrectomy was performed through

a 1.0 cm incision on left dorsolateral paralumbar region as follows (**Figure 4**). After skin incision, abdominal muscles were incised to expose retroperitoneal region. Left kidney was secured with a clamp (FRANCIS chalazion forceps, D-8425) and fat attached to kidney was removed. Special care was taken to prevent damage to the adrenal gland. Renal blood vessels and ureter were ligated with sterile silk surgical sutures (Deknatel^{R} Silk). Subsequently, left kidney was excised distal to ligatures. Abdominal muscles were sewn with reabsorbal thread (Vicryl* 5-0, ETHICON V303H) and opposite ends of incised skin was clipped together using sterile disposable skin staplers (3M Precise^{TM} REF. DS-25). Sham-operated control mice underwent identical surgical procedure except for kidney removal. Subcutaneous injection of buprenorphine (Essex, Luzern, Switzerland) every 6 hours for 2 days was used for analgesia. The mice were monitored until they recovered from anaesthesia and returned to its home cage.

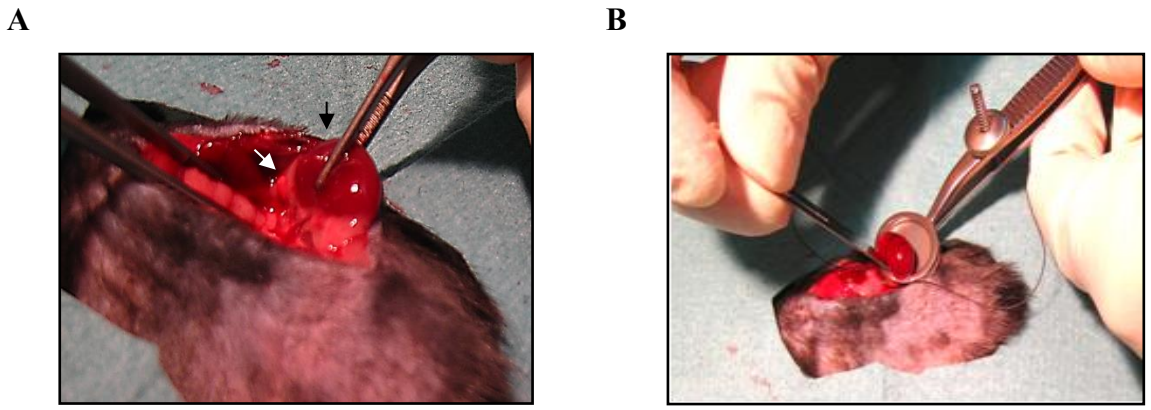

Figure 4 Surgical procedure of uninephrectomy. Left uninephrectomy was performed at 7 weeks of age. **A**: The left dorsolateral paralumbar region was opened. The left adrenal gland (white arrow) and the left kidney (black arrow) were visualized. **B**: Left kidney was secured with a clamp and was then excised distal to the ligature.

2.4 Maintenance of mice with telmisartan-treatment

After surgery, the HFD-fed mice were randomized to two groups. The mice were given either telmisartan (Boehringer Ingelheim International GmbH, MTA 1037) (~3mg/kg*day) in drinking water, or without any drug in drinking water for 20 weeks. The body weight of the animals was monitored once a week. To ensure the delivery of drug

doses, the concentrations of the drugs in drinking water were adjusted weekly according to the body weight and water assumption.

2.5 Intraperitoneal glucose and insulin tolerance tests

For intraperitoneal glucose tolerance test (ipGTT) mice were fasted overnight and for intraperitoneal insulin tolerance tests (ipITT) for 3 hours. Either glucose (2g/kg body weight) or human recombinant insulin (1.0 U/kg body weight) were injected intraperitoneally by a gavage needle (0.30mm (30G) x 8mm; BD Micro-Fine, Becton Dickinson, France) [144]. Blood glucose concentration was measured with a Glucometer (Contour Blutzuckermessgerät; Bayer HealthCare, Basel, Switzerland) with blood from tail-tip bleedings at different time points (i.e. 0, 15, 30, 45, 60, 90 and 120 minutes). Area under the curve (AUC) was calculated as changes from zero.

2.6 Hyperinsulinaemic-euglycaemic clamp

After mice were anaesthetized (as described previously in surgical procedure), a catheter for intravenous infusion of solution during clamp was inserted into the jugular vein in each mouse. After recovery from the intravenous catheterization surgery, glucose clamp studies were performed in freely moving mice 20 weeks after uninephrectomy. Glucose infusion rate was calculated once glucose infusion reached a more or less constant rate with blood glucose levels at 5 mmol/l (80–90 min after the start of insulin infusion). Thereafter, blood glucose was kept constant at 5 mmol/l for 20 min and glucose infusion rate was calculated [145]. The glucose disposal rate was calculated by dividing the rate of [3-^{3}H] glucose infusion by the plasma [3-^{3}H]glucose specific activity [146]. Endogenous glucose production during the clamp was calculated by subtracting the glucose infusion rate from the glucose disposal rate [146, 147]. Insulin-stimulated glucose disposal rate was calculated by subtracting basal endogenous glucose production (equal to basal glucose disposal rate) from glucose disposal rate during the clamp [148]. In order to assess tissue specific glucose uptake, a bolus (10 μCi) of 2-[1-^{14}C]deoxyglucose was administered via catheter at the end

of the steady state period. Blood was sampled 2, 15, 25 and 35 min after bolus delivery. Area under the curve of disappearing plasma 2-[1-^{14}C]deoxyglucose was used together with tissue-concentration of phosphorylated 2-[1-^{14}C]deoxyglucose to calculate glucose uptake [149].

2.7 Metabolic cage analysis

Eight metabolic cages in an open-circuit indirect calorimetric system were used (PhenoMaster, TSE Systems, Bad Homburg, Germany). Food and water intake, O_2 consumption, and CO_2 production were determined for single housed mice during a 24-h period as follows [150]. After being adapted to single caging, mice were placed in cages closed with air-tight lids. Water bottles and food cups were placed on scales to measure water and food intake continuously. The measurements were saved on a computer in 20 min intervals and were used to calculate cumulative food and water intake. Activity data were measured using an infrared light-beam. To measure energy expenditure (EE) and respiratory exchange ratio (RER), ambient air was pumped through the cage via a flow controller. Air entering and leaving each cage was monitored for its O2 and CO2 concentration. The cages were connected to two analysers measuring O2/CO2 concentration of each cage for a period of 2 min in 20 min intervals. EE and RER were calculated using the manufacturer's software based on the following equation: EE (kcal/h) = (3.941×VO2+1.106×VCO2)/1000; RER=VCO2/VO2.

2.8 Determination of insulin, free fatty acid, angiotensin I, creatinine, uric acid and bile acid levels

Plasma was collected from the tail vein after 7 hours of fasting. Insulin was determined using an ELISA kit (Ultra Sensitive Rat Insulin ELISA; Crystal Chem, Downers Grove, IL, USA). Free fatty acid levels were measured using the ACS-ACOD-MEHA method (Wako Chemicals GmbH, Neuss, Germany). Plasma angiotensin I levels

were determined by an ELISA kit (Cusabio Biotech CO Ltd, Wuhan, PR China). Serum creatinine levels were measured using DetectX® Low Sample Volume Serum Creatinine Kit (K0021-H1D, Arbor Assays, Ann Arbor, MI, USA), serum uric acid levels by QuantiChrom™ Uric Acid Assay Kit (DIUA-250, BioAssay Systems, Hayward, CA, USA) and plasma bile acid levels using Mouse Total Bile Acids Assay Kit (80470, Crystal Chem Inc, Downers Grove, IL, USA).

2.9 Total liver lipid extraction

Liver tissue (30 mg) was homogenized in PBS, and lipids were extracted in a chloroform/methanol (2:1) mixture. Total liver lipids were determined by a sulfo-phospho-vanillin reaction as described by Knight et al. [151]. The liver lipid samples were heated at 90^0C on heating block until dry and then cooled down on ice. Sulphuric acids were added to the samples and boiled at 90^0C in water bath for 10 min and cooled down on ice. Vanillin-reagent was added to the samples and incubated for 40 min at room temperature. Samples were transferred to a 96 well plate and detected by an Elisa-reader at 550 nm.

2.10 Glucose incorporation into isolated soleus and EDL muscle

Mice were fasted for 4 hours prior to the analysis. Extensor digitorum longus (EDL) and soleus muscles were removed from anesthetized mice (Avertin, 99% 2,2,2-tribromo ethanol, and tertiary amyl alcohol at 15–17 μl/g body weight i.p.) and incubated for 30 min at 30^0C in vials containing preoxygenated (95% O_2-5% CO_2) Krebs-Henseleit buffer (KHB) containing 5 mM HEPES (prebuffer) and supplemented with 15 mM mannitol and 5 mM glucose. Muscles were transferred to new vials containing fresh pre-gassed KHB, as described above, in the absence or presence 120nM of insulin (Actrapid; Novo Nordisk, Mainz, HE, Germany). Afterwards, muscles were transferred to new vials containing preoxygenized KHB supplemented with 20 mM mannitol and incubated for 10 min. Muscles were then transferred to new vials containing preoxygenized KHB supplemented with 1 mM [^{3}H]2-deoxy-glucose (2.5 μCi/ml), and 19mM [^{14}C]mannitol to account for

extracellular space, and incubated for 20 min. After the last incubation, muscles were washed in ice-cold KHB, dried externally on filter paper, and quickly frozen with aluminium tongs precooled in liquid nitrogen and stored at −80°C. Glucose transport rates were determined by scintillation counting of cleared protein lysates as described [152].

2.11 Insulin signalling in skeletal muscle *ex vivo*

For assessing insulin-stimulated Akt phosphorylation in skeletal muscle, insulin (2U/kg) was injected intraperitoneally in mice fasted for 5 hours. Skeletal muscles (quadriceps) were harvested 15 minutes after insulin injection, snap frozen in liquid nitrogen and stored at -80°C until homogenization. Samples were further assessed by Western blotting.

2.12 Histology

Epididymal fat tissues were fixed in 4% buffered formalin and embedded in paraffin. Sections were cut and stained with hematoxylin and eosin. After slides were air-dried, 1-2 drops immu-Mount were added and then cover slip was applied. For each fat pad at least 100 adipocytes were analysed. Quadriceps femoris muscle was mounted in embedding medium (o.c.t. embedding matrix, CellPath Ltd., Newtown, UK), snap frozen in isopentane cooled to -160°C with liquid nitrogen, and subsequently stored at -80°C until use. Consecutive 12 µm sections were cut on a microtome at -25°C. Rat anti-mouse CD31 endothelial cell antibody (BioLegend, San Diego, CA) was used as a marker for muscle capillaries, and capillary-to-fiber ratio was calculated by dividing the number of CD31-positive cells by the number of muscle fibers. For all histochemical and immunohistochemical analyses NIH Image J software (National Institutes of Health, Bethesda, MD, USA) was used.

2.13 RNA extraction and quantitative rt-PCR

Total RNA was extracted with the RNAeasy Lipid Tissue Mini Kit (Qiagen). RNA was analysed with a Bioanalyzer (Agilent Technologies, Santa Clara, CA, USA) and concentration was determined with a nanodrop. RNA (0.75 μg) was reverse transcribed with Superscript III Reverse Transcriptase (Invitrogen) using random hexamer primers (Invitrogen). TaqMan system (Applied Biosystems) was used for real-time PCR amplification. The amplification consisted of a 2 min period at 50^0C to activate the Uracil-N-Glycosylase. Samples were heated to 95^0C followed by 40 cycles with denaturation at 95^0C for 14 seconds and annealing/elongation at 60^0C for 1 minute. Relative gene expression was obtained after normalization to 18s RNA (Applied Biosystems), using the formula 2-ΔΔcp [153]. The following primers were used: TNF-α Mm00443258_m1, IL-6 Mm00446190_m1, IL-1β Mm0043422/8_m1, CD11c Mm00498698_m1, ATGL Mm00503040_m1, perilipin Mm00558672_m1, HIF1α Mm00468869_m1, CD31 Mm01242584_m1 (Applied Biosystems, Rotkreuz, Switzerland).

2.14 Western blotting

Cells or tissues were lysed in ice-cold lysis buffer containing 150 mM NaCl, 50 mM Tris-HCI (pH 7.5), 1 mM EGTA, 1% NP-40, 0.25% sodium deoyxcholate, 1 mM sodium vanadate, 1 mM NaF, 10 mM sodium β-glycerolphosphate, 100 nM okadaic acid, 0.2 mM PMSF and a 1:1000 dilution of protease inhibitor cocktail (Sigma-Aldrich). Protein concentration was determined using a BCA assay (Pierce, Rockford, IL, USA). Equivalent amounts of protein (20-50 g) were resolved by LDS-PAGE (4%-12% gel; NuPAGE, Invitrogen, Basel, Switzerland). Proteins were electro-transferred to a nitrocellulose membrane (0.2 μm, BioRad, Reinach, Switzerland) and blocked for 1 hour in 5% non-fat dry milk (BioRad) resolved in Tris-buffer saline, containing 1% Tween-20. Membranes were incubated overnight at 4^o C on a rocking platform with respective primary antibodies. The following primary antibodies were used: anti-phospho-Akt (Ser473) (Cell Signalling, Danvers, MA, USA) and anti-actin (Millipore, Zug, Switzerland).

Subsequently, membranes were incubated with secondary antibody (HRP-conjugated; Santa Cruz Biotechnology and Alexis Biochemicals) for 1 hour at room temperature. Signals were generated after 5 minutes incubation with Lumi-Light chemoluminiscence (Roche). Membrane was exposed and signals were detected in an Image Analyser (FujiFilm) [153].

2.15 Data analysis

Data are presented as mean +/- SEM and were analyzed by unpaired Student's t test. P-values < 0.05 were considered significant.

3 Results

3.1 General adaptations of UniNx and sham-operated mice to surgical intervention

3.1.1 Similar body weight in sham-operated and UniNx mice

Dependent on the surgical intervention, mice were divided into two groups: sham-operated or UniNx mice. Mice were then fed either a chow or high-fat diet (HFD) for up to 20 weeks. Body weight was determined in weekly intervals. As expected, body weight gain of HFD-fed animals was significantly higher than that of chow-fed mice. Uninephrectomy had no significant influence on body weight neither in HFD-fed nor in chow-fed mice. However, there was a tendency towards decreased weight gain in UniNx mice as compared to sham-operated mice under both chow and HFD (**Figure 5**).

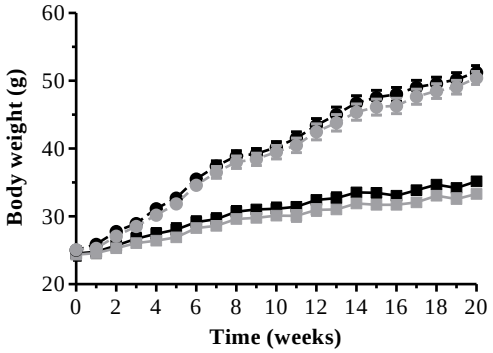

Figure 5 Body weights of uninephrectomised (UniNx) and sham-operated mice. Results are means and SEM of 7 to 17 animals per group. *p < 0.05 (Student's t test). ■ Sham chow; ■ UniNx chow; ● sham HFD; ● UniNx HFD.

3.1.2 Increased epididymal fat pad weight in HFD-fed UniNx mice

After 20 weeks of surgery, remnant kidneys of both chow and HFD-fed UniNx mice were heavier compared to sham-operated mice. Liver weights of HFD-fed animals

were significantly heavier than those of chow-fed mice. However, no difference in liver weights were observed between sham-operated and UniNx mice (**Figure 6A**). In HFD-fed animals, epididymal fat pad weight was significantly higher in UniNx mice, whereas inguinal and mesenteric fat pad weights were similar in HFD-fed UniNx and sham-operated mice. No differences in fat pad weights were observed in chow-fed mice (**Figure 6B**).

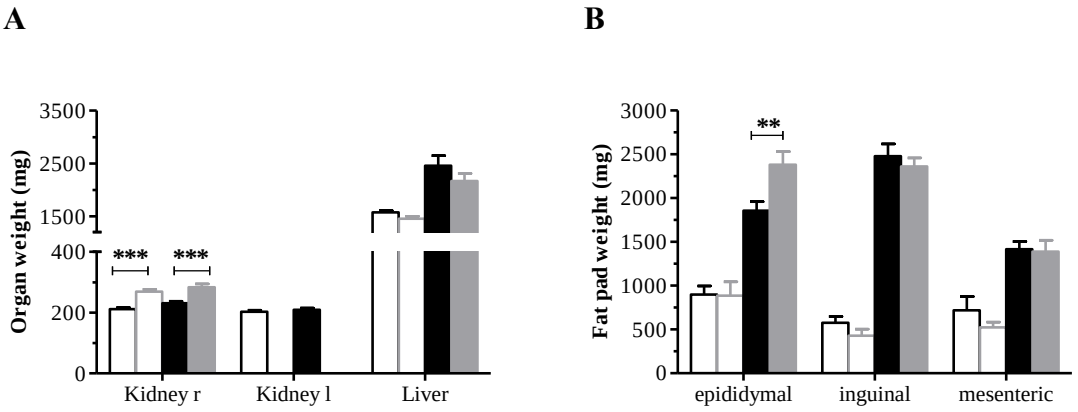

Figure 6 Organ weights were assessed 20 weeks after surgery. (**A**) Absolute weight of kidneys (r: right; l: left) and livers of HFD-fed sham-operated and UniNx mice are depicted. (**B**) Different fat pads were harvested and weighed. Results are means and SEM of 7 to 13 animals per group. **p < 0.01, ***p < 0.001 (Student's t test). ☐ Sham chow; ☐ UniNx chow; ■ sham HFD; ■ UniNx HFD.

3.1.3 Similar food intake, locomotion and respiratory quotient in sham-operated and UniNx mice

Food intake, locomotion, and fuel utilization (respiratory quotient, RQ) were determined in metabolic cages. As depicted in **Figure 7**, these parameters were similar between HFD-fed sham-operated and UniNx mice.

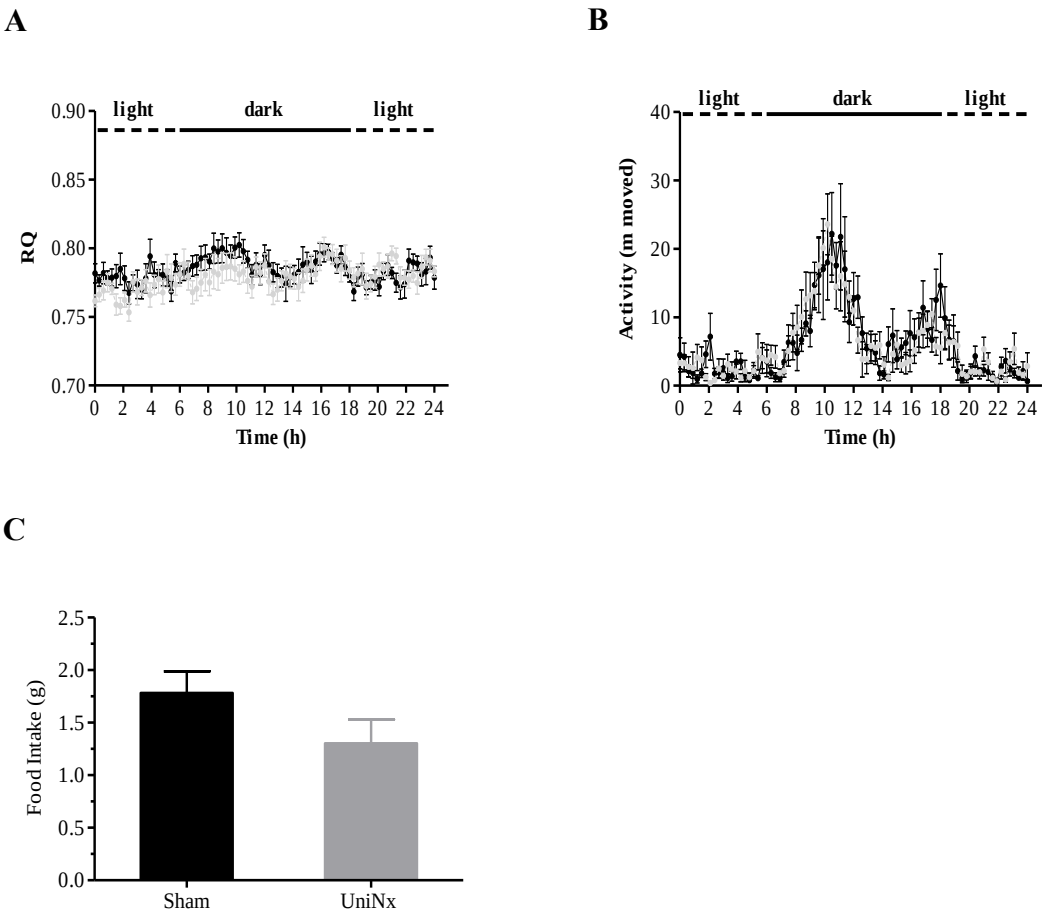

Figure 7 Metabolic cage analyses. Respiratory quotient (RQ) (**A**), locomotor activity (**B**) and food intake (**C**) was determined in HFD-fed sham-operated (black symbols) and UniNx (grey symbols) mice. n=7-8. Error bars represent SEM.

3.1.4 Similar circulating blood metabolites in sham-operated and UniNx mice

Fasting blood glucose levels, as readout for hepatic glucose production, were similar in HFD-fed sham-operated and UniNx mice (**Table 2**). Interestingly, plasma insulin levels were significantly lower in chow-fed UniNx compared to sham-operated mice, whereas no such difference was observed in HFD-fed mice. In addition, plasma free fatty acids (FFAs) concentrations did not differ significantly between both groups 20 weeks after surgery. Similarly, bile acids levels were not different between sham-operated and UniNx mice. Additionally, uric acid levels were comparable between HFD-fed sham-operated and UniNx mice.

	Sham-operated		UniNx	
	Chow	HFD	Chow	HFD
Glucose (mmol/l)	7.8 ± 0.7	11.7 ± 0.8$^{\#\#}$	8.8 ± 0.4	11.9 ± 0.8$^{\#\#}$
n	*7*	*10*	*8*	*10*
Insulin (ng/ml)	1.6 ± 0.2	7.0 ± 0.6$^{\#\#\#}$	0.9 ± 0.1**	5.9 ± 0.8$^{\#\#\#}$
n	*7*	*10*	*8*	*10*
FFA (mmol/l)	n.d.	0.72 ± 0.9	n.d.	0.79 ± 0.9
n		*5*		*5*
Uric acid (mg/dl)	n.d.	4.4 ± 0.4	n.d.	5.4 ± 0.8
n		*8*		*9*
Bile acids (µmol/l)	8.4 ± 3.1	9.4 ± 1.3	8.2 ± 2.3	14.0 ± 4.0
n	*7*	*10*	*8*	*10*

Table 2 Circulating blood parameters in sham-operated and UniNx mice. Results are means and SEM of 7 to 17 animals per group. *p<0.05, **p<0.01, ***p<0.001 compared to sham-operated mice; $^{\#}$p<0.05, $^{\#\#}$p<0.01, $^{\#\#\#}$p<0.001 compared to chow-fed mice; n.d. - not determined

3.1.5 Increased circulating creatinine and cystatin C levels in HFD-fed UniNx mice

Twenty weeks after surgery, serum creatinine levels in HFD-fed UniNx mice were slightly, but significantly increased (**Figure 8A**). Nonetheless, the increased creatinine concentration in UniNx mice was still within normal limits. Of note, normal creatinine levels in mice range from 0.164 to 0.942 mg/dl. Cystatin C levels, which is a more accurate readout for glomerular infiltration rate (GFR) than serum creatinine, were significantly higher in HFD-fed UniNx mice (**Figure 8B**) suggesting decreased GFR in HFD-fed UniNx compared to sham-operated mice.

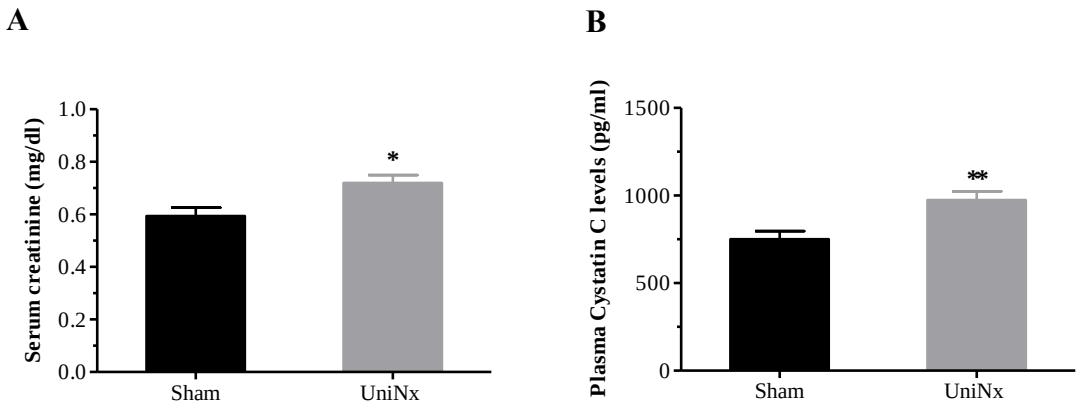

Figure 8 Increased creatinine and cystatin C levels in HFD-fed UniNx mice. Serum creatinine (**A**) and plasma cystatin C (**B**) were determined 20 weeks after surgery in HFD-fed sham-operated (black bars) and UniNx mice (grey bars) mice. n=6-9. *p < 0.05, **p < 0.01 (Student's t test). Error bars represent SEM.

3.2 Similar overall insulin sensitivity and glucose tolerance in HFD-fed UniNx and sham-operated mice

Intraperitoneal glucose and insulin tolerance tests were performed 2, 8 and 20 weeks after surgical intervention in chow- and HFD-fed sham-operated and UniNx mice. In chow-fed animals, glucose and insulin tolerance tests were similar at all time points evaluated (**Figure 9**). Interestingly though, there was an unexpected trend towards improved glucose tolerance in chow-fed UniNx compared to sham-operated mice 20 weeks after surgery (**Figure 9Aiii**). HFD-fed mice showed the expected deterioration in glucose and insulin tolerance. However, glucose and insulin tolerance tests were not different between HFD-fed sham-operated and UniNx mice except for slightly higher glucose levels in UniNx mice after 8 weeks of HFD (**Figure 9Aii**).

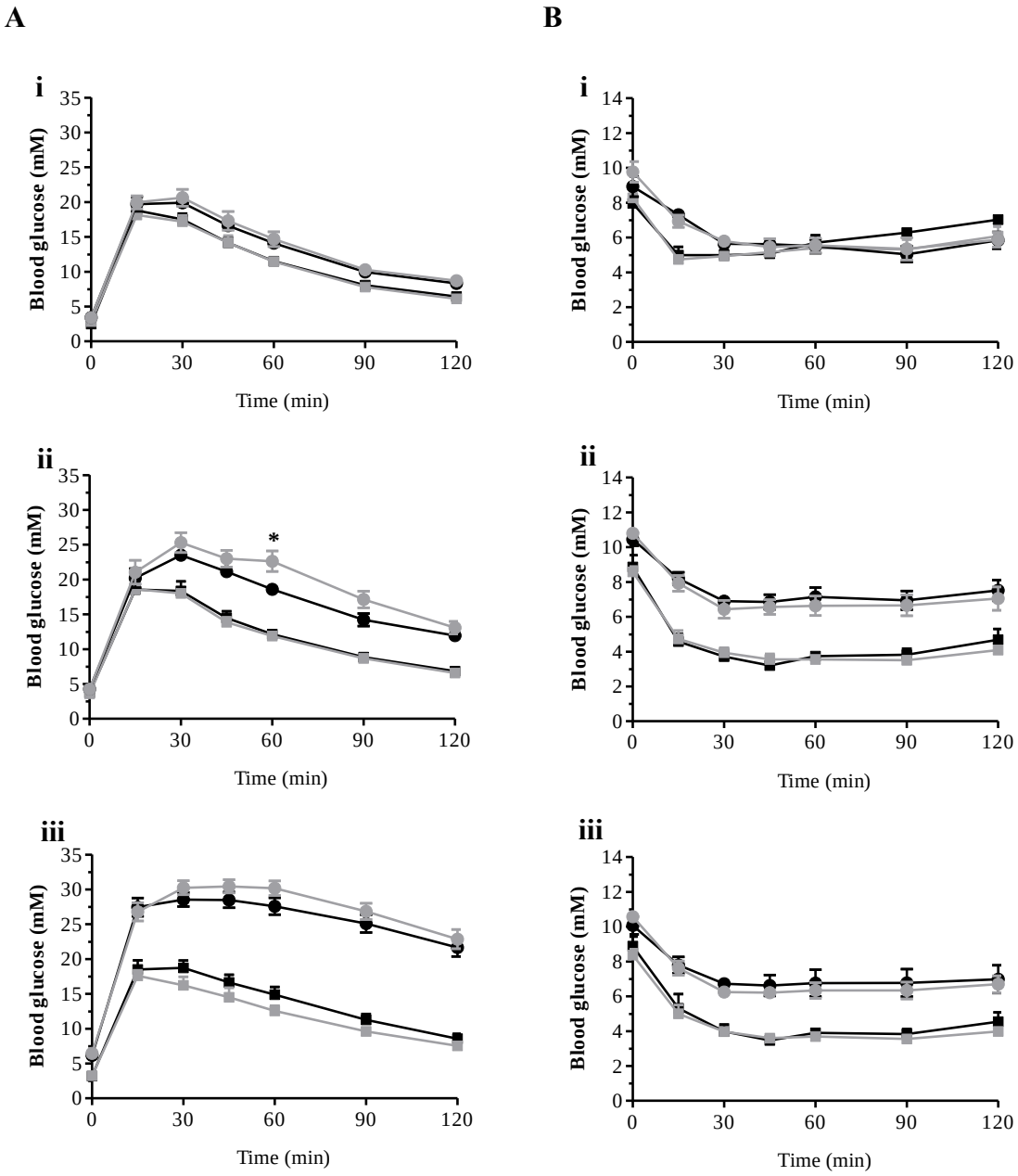

Figure 9 Similar overall insulin sensitivity and glucose tolerance in UniNx mice compared to sham-operated mice. Intraperitoneal glucose tolerance test (**A**) and insulin tolerance test (**B**) were performed at (**i**) 2, (**ii**) 8, (**iii**) 20 weeks after surgery. Results are means and SEM of 7 to 17 animals per group. *p < 0.05, **p < 0.01 (Student's t test). ■ Sham chow; ■ UniNx chow; ● sham HFD; ● UniNx HFD.

In order to more accurately determine insulin sensitivity, hyperinsulinaemic-euglycaemic clamp studies were performed in HFD-fed mice 20 weeks after surgery. As depicted in **Figure 10B** and **10C**, overall (total body) insulin sensitivity was similar between HFD-fed sham-operated and UniNx mice.

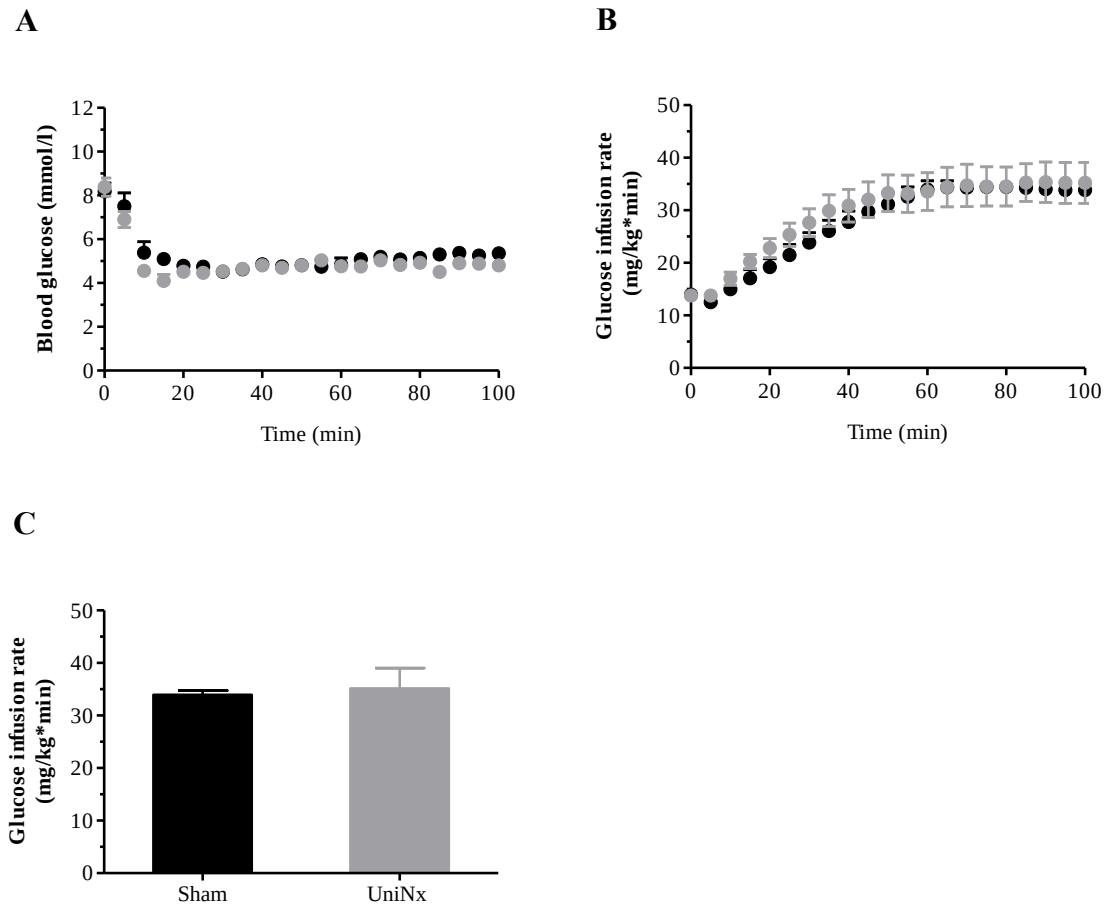

Figure 10 Blood glucose concentrations and glucose infusion rates during hyperinsulinaemic-euglycaemic clamp. (**A**) Blood glucose levels were clamped upon insulin infusion at about 5 mmol/l in HFD-fed sham (black symbols) and UniNx (grey symbols) mice. (**B**) In order to maintain euglycaemia, glucose infusion rate was adjusted over time. (**C**) Glucose infusion rate (GIR) during hyperinsulinaemic-euglycaemic clamps. Results are the mean ± SEM of 5 animals per group.

3.3 Improved hepatic but deteriorated muscle insulin sensitivity in HFD-fed UniNx mice

Endogenous glucose production (EGP), mainly reflecting hepatic glucose production, was determined during hyperinsulinaemic-euglycaemic clamp. As depicted in **Figure 11A**, insulin-induced suppression of EGP was blunted in HFD-fed sham-operated mice, but clearly evident in HFD-fed UniNx mice indicating improved/preserved hepatic insulin sensitivity in HFD-fed UniNx mice. In contrast, insulin-stimulated glucose disposal rate (IS GDR), mainly reflecting insulin-stimulated glucose disposal, was significantly

reduced by more than 50% in HFD-fed UniNx mice, suggesting that UniNx further deteriorated HFD-induced skeletal muscle insulin resistance (**Figure 11B**).

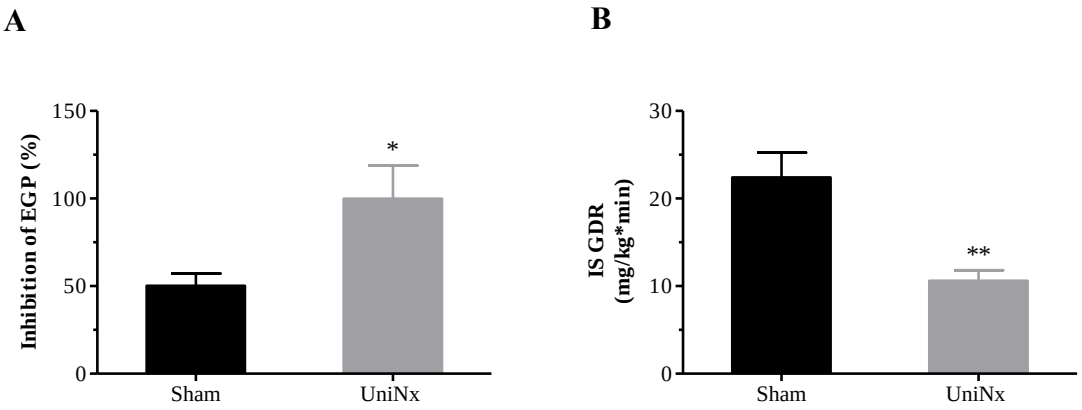

Figure 11 Improved hepatic but deteriorated muscle insulin sensitivity in HFD-fed UniNx mice. Hyperinsulinaemic-euglycaemic clamp studies were performed in HFD-fed sham-operated (black bars) and uninephrectomised (grey bars) mice 20 weeks after surgery. Insulin-mediated inhibition of endogenous glucose production (EGP) corresponding to hepatic insulin sensitivity is depicted in (**A**). Insulin-stimulated glucose disposal rate (IS GDR) reflecting muscle insulin sensitivity is shown in (**B**). Results are the mean ± SEM of 5 animals per group. *p < 0.05, **P < 0.01 (Student's t test).

3.4 Improved hepatic steatosis in HFD-fed UniNx mice

Consistent with improved hepatic insulin sensitivity (**Figure 11A**), total liver lipid content was greatly reduced in HFD-fed UniNx compared to sham-operated mice (**Figure 12A)**. Such result was supported by histological examination of liver sections revealing higher numbers of lipid vacuoles in HFD-fed sham-operated mice (**Figure 12B**).

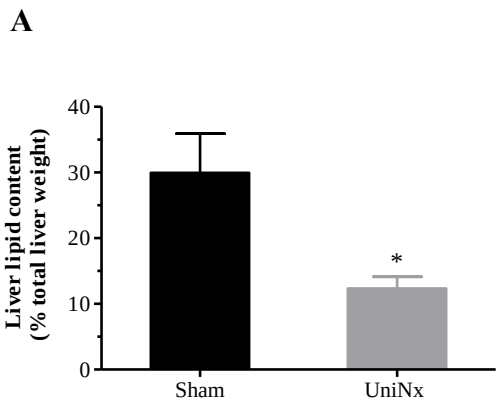

B

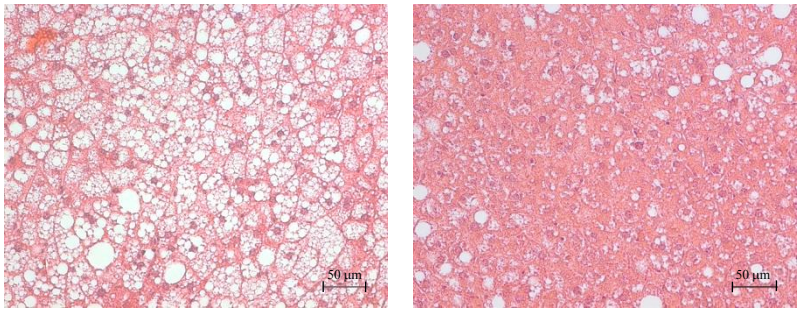

Sham UniNx

Figure 12 Improved hepatic steatosis in HFD-fed UniNx mice. (**A**) Total liver lipids were determined and expressed relative to total liver in HFD-fed sham-operated (black bar) and uninephrectomised (grey bar) mice 20 weeks after surgery. (**B**) Representative hematoxylin-eosin stained histological sections of liver of HFD-fed sham-operated and UniNx mice. Scale bar represent 50 µm. Results are the mean ± SEM of 5-7 animals per group. *p < 0.05 (Student's t test).

3.5 Reduced adipose tissue inflammation in HFD-fed UniNx mice

The 'portal theory' proposes that the direct exposure of the liver to increasing amounts of FFAs and/or pro-inflammatory factors released from visceral fat into the portal vein may promote the development of hepatic insulin resistance and steatosis [23]. Accordingly, mRNA expression of pro-inflammatory cytokines as well as adipose tissue histology was analysed in order to characterize adipose tissue inflammation. As depicted in **Figure 13A**, expression of CD11c (a marker for pro-inflammatory M1 polarized macrophages) and IL-6 was significantly decreased and expression of TNFα and IL-1β trendwise reduced in mesenteric adipose tissue of HFD-fed UniNx compared to sham-operated mice. Of note, mRNA levels of the hypoxia-inducible factor 1-alpha (HIF1α) was significantly lower in mesenteric adipose tissue of HFD-fed UniNx mice. Histologically, obesity is associated with macrophage infiltration in adipose tissue and these macrophages seem to form so called crown-like structures by surrounding mainly necrotic, hypertrophic adipocytes. In obese sham-operated mice, macrophages and crown-like structures were easily detected in HFD-fed sham-operated mice, whereas, they were less prominent in HFD-fed UniNx mice (**Figure 13B**). In contrast, adipocyte diameter was not different

between both groups of mice (**Figure 13C**). Moreover, insulin-stimulated Akt-phosphorylation in adipose tissue was similar in both groups suggesting similar insulin sensitivity in these tissues (**Figure 13D**). Thus, in addition to improved/preserved hepatic insulin sensitivity, uninephrectomy protects mice from the development of HFD-induced adipose tissue inflammation.

A

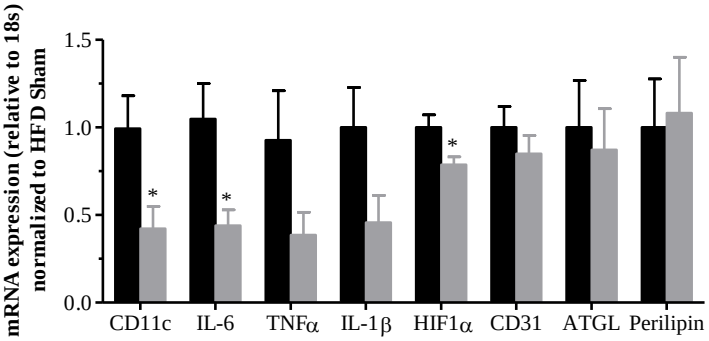

B

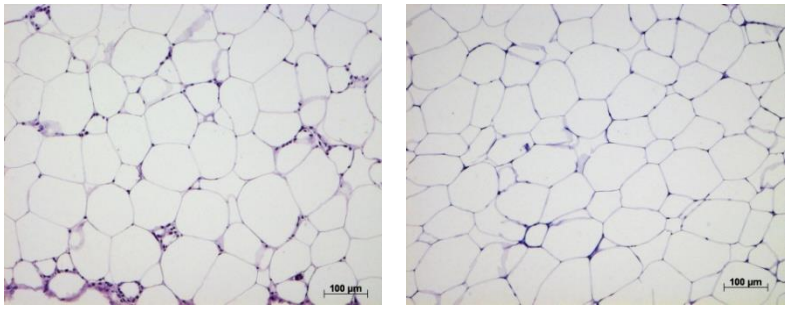

C

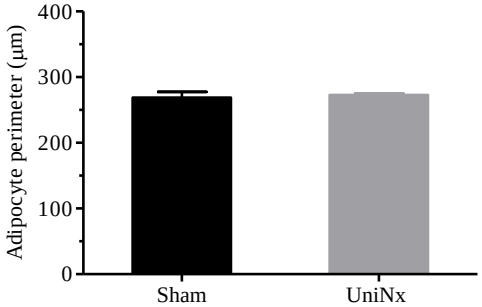

D

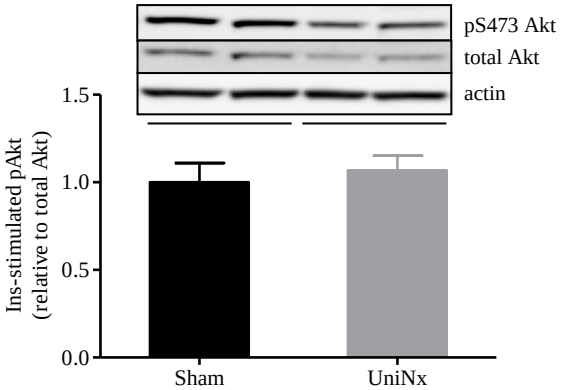

Figure 13 Reduced adipose tissue inflammation in HFD-fed UniNx mice. (**A**) mRNA expression of respective genes in mesenteric adipose tissue of HFD-fed sham-operated (black bars) and uninephrectomised (grey bars) mice 20 weeks after surgery, n=5-10. *p < 0.05 (Student's t test). (**B**) Representative hematoxylin-eosin stained histological sections of epididymal adipose tissue of HFD-fed sham-operate and UniNx mice. (**C**) Adipocyte cell perimeter was measured by using Image J. Up to 100 cells per fat pad of four different mice per group was analysed. All values are expressed relative to the adipocyte cell perimeter of HFD-fed sham-operated mice. Scale bar represent 100 μm. (**D**) Lysates of white adipose tissue were prepared, resolved by LDS-PAGE and immunoblotted with anti-pS473AKT, anti-total Akt or anti-actin antibody. Graphs from **B** to **D** show results of 4-5 mice. Results are the mean ± SEM. (ATGL: adipose triglyceride lipase)

3.6 Similar skeletal muscle insulin action *ex vivo*

Glucose uptake into isolated soleus (slow-twitch) and extensor digitorum longus (fast-twitch) muscles was assessed next removing extramyocellular barriers to muscle glucose uptake. As depicted in **Figure 14A** and **14B**, basal and insulin-stimulated glucose uptake were similar between HFD-fed sham and UniNx mice, suggesting no direct impairment of insulin action at the myocyte level. Of note, 20 weeks of HFD led to an expected poor insulin response in skeletal muscle, which was particularly evident in soleus muscle. Similarly, no difference between both groups of mice was found for *ex vivo* insulin-stimulated Akt phosphorylation (**Figure 14C**) in total muscle homogenates. These data in isolated muscle contrast the data obtained from hyperinsulinaemic-euglycaemic clamp studies revealing diminished muscle insulin sensitivity in HFD-fed UniNx mice (**Figure 11B**) and may indicate that UniNx leads to impaired insulin delivery to the sarcolemma, e.g. through reduction in capillary density.

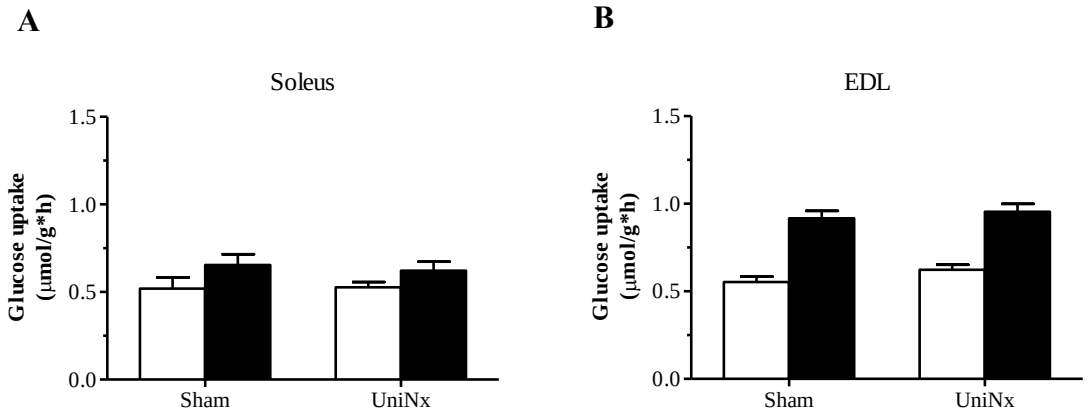

C

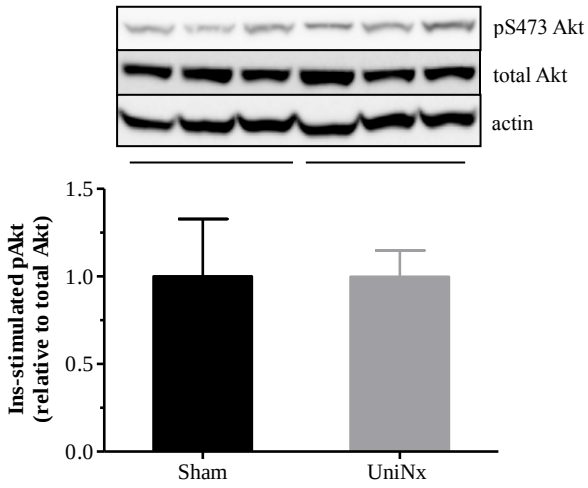

Figure 14 Preserved/sustained insulin-stimulated glucose uptake into skeletal muscle *ex vivo* in HFD-fed UniNx mice. Glucose uptake into intact isolated soleus muscle (**A**) and extensor digitorum longus (EDL) (**B**) was measured in the absence or presence of 120 nM insulin. n=8. Basal state (open bars), insulin-stimulated state (black bars). (**C**) Total muscle lysates were prepared, resolved by LDS-PAGE and immunoblotted with anti-pS473 Akt, anti-total Akt or anti-actin antibody. Graphs show results of 4-5 mice.

3.7 Reduced capillary density in skeletal muscle of HFD-fed UniNx mice

In order to assess capillary density, expression of the endothelial marker CD31 was determined. As depicted in **Figure 15A**, mRNA levels of CD31 were significantly reduced in quadriceps muscle in HFD-fed UniNx compared to sham-operated mice. Moreover, capillary-to-fiber ratio was significantly (~15%) reduced in skeletal muscle of HFD-fed UniNx mice (**Figure 15B** and **C**). These results suggest that uninephrectomy leads to a reduction in muscle capillary density in HFD-fed mice.

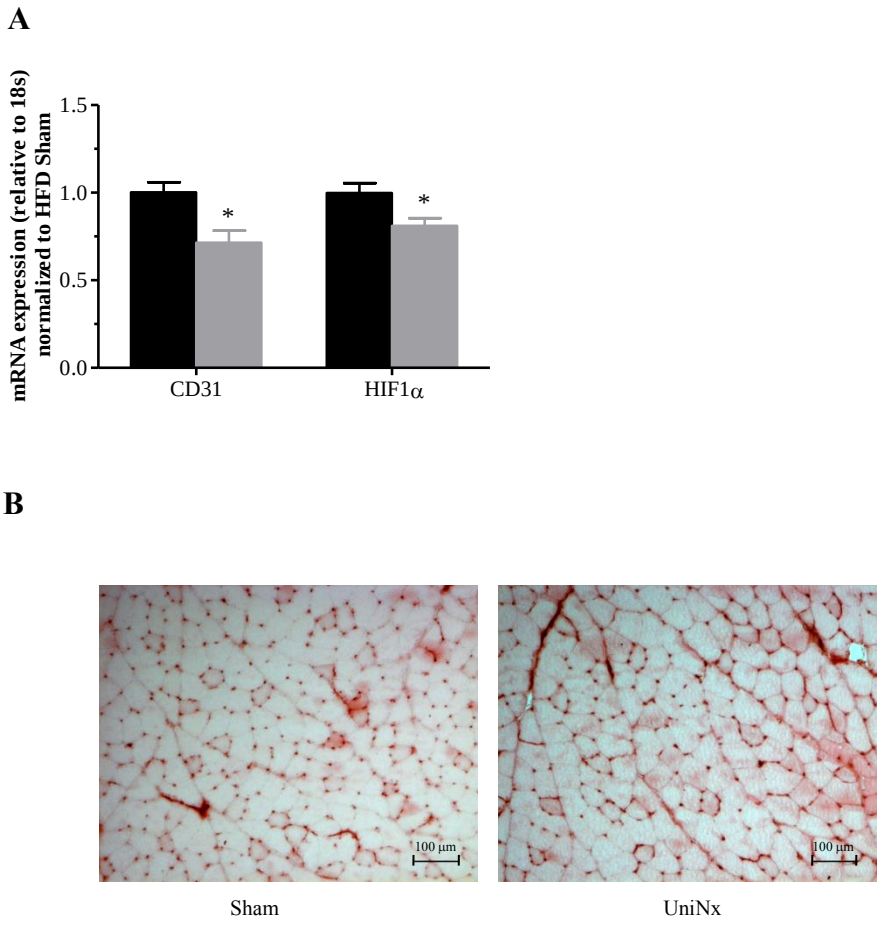

Figure 15 Reduced capillary density in skeletal muscle of HFD-fed UniNx mice. (**A**) mRNA expression of CD31 and HIFα in quadriceps muscle of HFD-fed sham-operated (black bars) and UniNx mice (grey bars). n=4-5. (**B** and **C**) CD31 staining of quadriceps muscle isolated from HFD-fed sham-operated and UniNx mice. Capillary-to-fiber ratio was calculated after counting up to 700 fibers and corresponding capillaries per mouse. n=4. Error bars represent SEM. *$p < 0.05$ (Student's t test).

3.8 Increased plasma angiotensin I levels in UniNx mice

As outlined in the introduction, activation of the renin-angiotensin-system (RAS) may contribute to HFD/obesity-induced insulin resistance. In addition, UniNx-induced reduction in kidney mass may result in increased angiotensin levels; and thus may contribute to observed deterioration of skeletal muscle insulin resistance [154-156]. Indeed, plasma angiotensin I level was elevated in UniNx compared to sham-operated mice under both chow and HFD 2, 8 and 20 weeks after surgical intervention (**Figure 16**) (data not shown for time points 2 and 8 weeks).

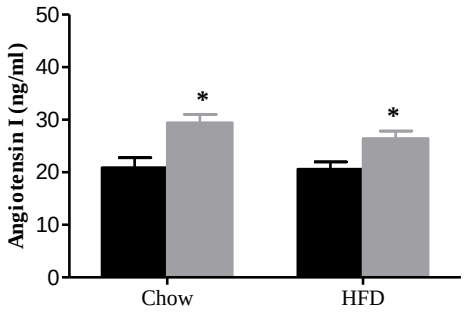

Figure 16 Increased angiotensin I levels in UniNx mice. Plasma angiotensin I levels were determined in sham-operated (black bars) and UniNx mice (grey bars) 20 weeks after surgery. Results are the mean ± SEM of 8 animals per group. *$p < 0.05$ (Student's t test).

3.9 Improved glucose tolerance in telmisartan-treated HFD-fed sham-operated mice

Since it was postulated that inappropriate activation of the renin-angiotensin system (RAS) induces HFD-associated skeletal muscle insulin resistance, we hypothesized that the observed increase in circulating angiotensin I concentration deteriorates HFD-induced skeletal muscle insulin resistance via activation of angiotensin II type 1 receptor (AT1R). To test such hypothesis we made use of the AT1R blocker telmisartan. UniNx and sham-operated mice were fed a HFD for 20 weeks and received telmisartan in the drinking water at a dose of 3mg/kg*day during the entire period. As depicted in **Figure 17A**, telmisartan-treated HFD-fed sham-operated mice gained much less body weight than untreated controls

and telmisartan-treated HFD-fed UniNx mice. Nevertheless, body weight gain in the latter mice was reduced compared to untreated UniNx controls (**Figure 17A**). Moreover, telmisartan treatment improved glucose tolerance in HFD-fed sham-operated but not UniNx mice (**Figure 17B** and **C**).

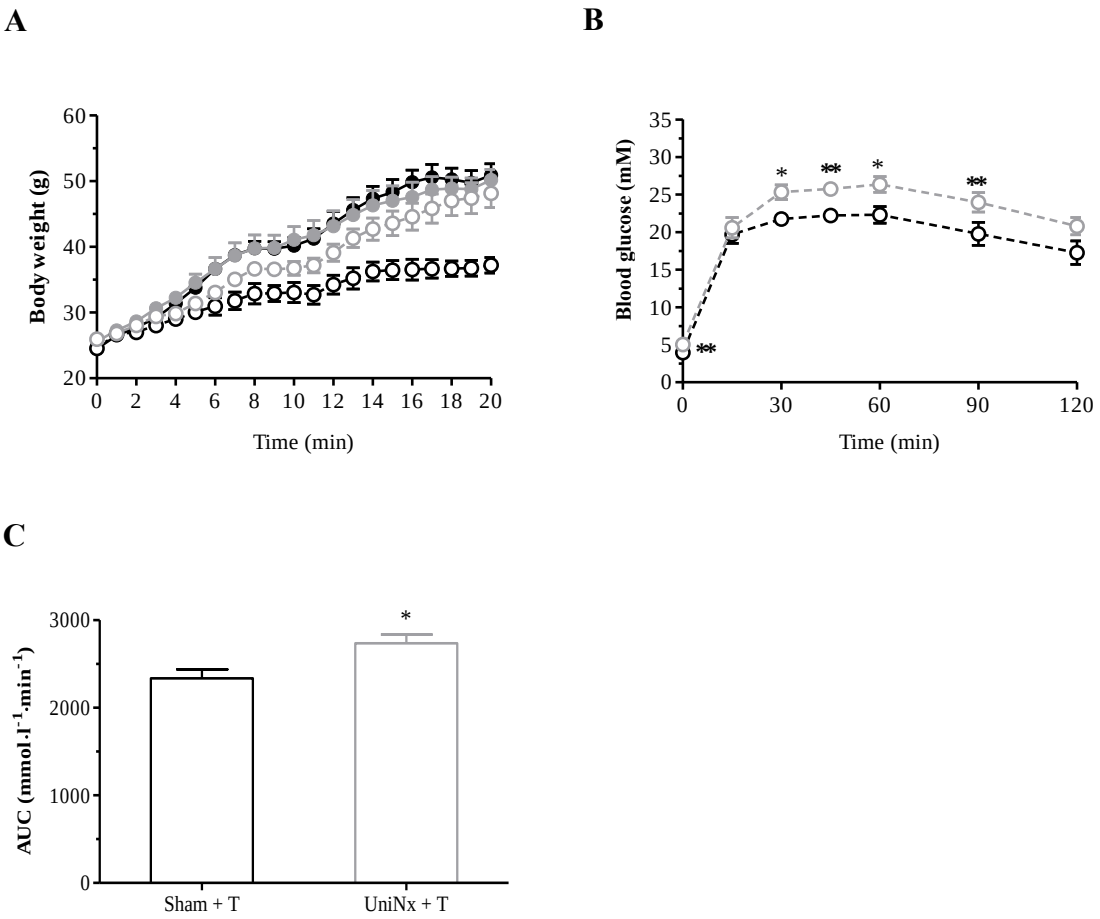

Figure 17 Telmisartan improves glucose tolerance in HFD-fed sham-operated mice. (**A**) Body weights of uninephrectomised (UniNx) and sham-operated mice. n=5. ● Sham HFD; ● UniNx HFD; ○ Telmisartan-treated sham HFD; ○ Telmisartan-treated UniNx HFD. (**B**) Intraperitoneal glucose tolerance test in telmisartan-treated HFD-fed sham-operated and UniNx mice. n=11. (**C**) Analysis of area under the curve of glucose tolerance tests presented in **B.** All error bars represent SEM.

3.10 Improved hepatic insulin sensitivity in telmisartan-treated HFD-fed sham-operated mice

In addition to glucose tolerance test, we next determined insulin sensitivity in telmisartan-treated HFD-fed mice by means of hyperinsulinaemic-euglycaemic clamp

study. As depicted in **Figure 18A**, glucose infusion rate was elevated in telmisartan-treated HFD-fed sham-operated mice indicating that telmisartan ameliorated total body insulin sensitivity in HFD-fed sham-operated mice. In contrast, glucose infusion rate (GIR) in telmisartan-treated HFD-fed UniNx was comparable to the rate observed in untreated HFD-fed UniNx controls (GIR in telmisartan-treated HFD-fed UniNx mice (**Figure 18A**): 45.1 ± 3.5 mg/kg*min; GIR in untreated HFD-fed UniNx mice (**Figure 10C**): 35.1 ± 3.9 mg/kg*min; p=0.10). Particularly, telmisartan improved insulin-induced suppression of hepatic glucose production in HFD-fed sham-operated mice, whereas rate of insulin-induced EGP-suppression was similar in telmisartan-treated and untreated HFD-fed UniNx mice (**Figure 18B** and **Figure 11A**).

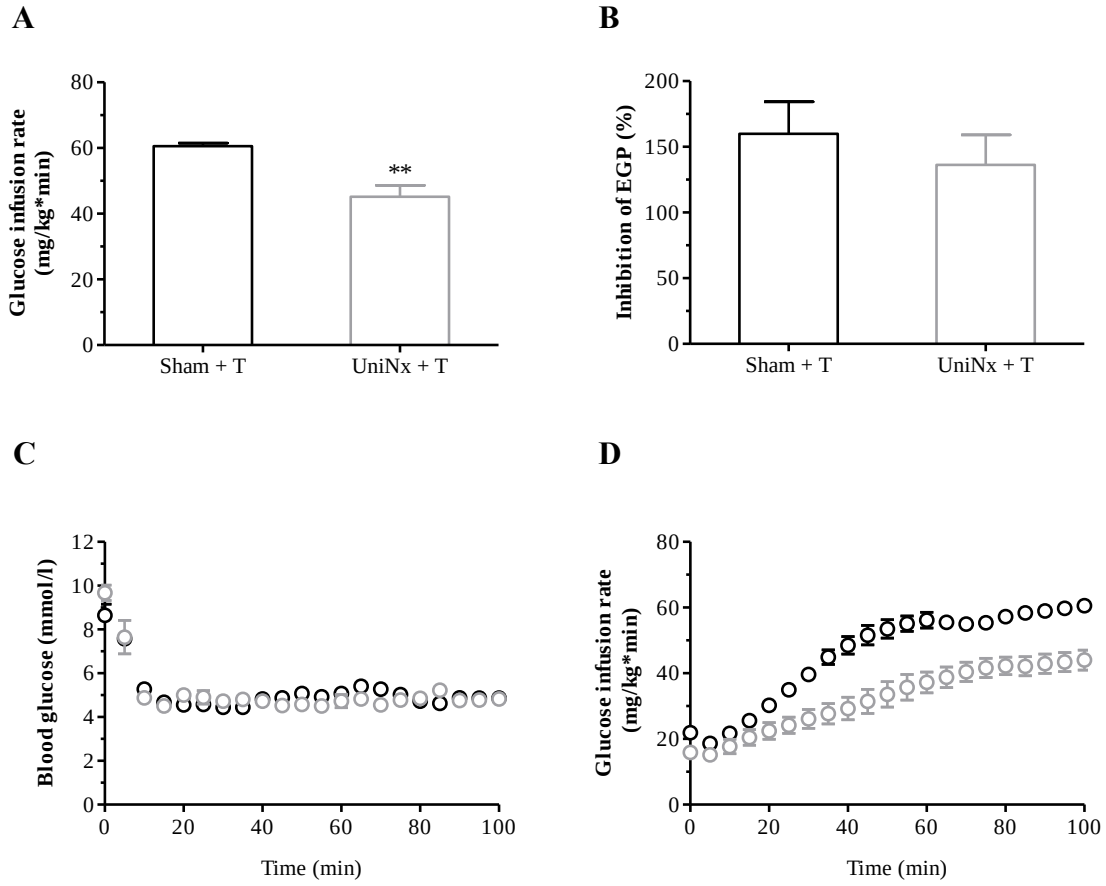

Figure 18 Telmisartan improves hepatic insulin sensitivity in HFD-fed sham-operated mice. (**A**) Glucose infusion rate (GIR) and (**B**) insulin-mediated inhibition of endogenous glucose production corresponding to hepatic insulin sensitivity. (**C**) Blood glucose levels were clamped upon insulin infusion at about 5 mmol/l in telmisartan-treated HFD-fed sham (black circles) and UniNx (grey circles) mice. (**D**) In order to maintain euglycaemia, glucose infusion rate was adjusted over time. n=5. All error bars represent SEM.

3.11 Improved hepatic steatosis in telmisartan-treated HFD-fed sham-operated mice

In accordance with elevated hepatic insulin sensitivity, telmisartan treatment reduced hepatic steatosis in sham-operated mice (total liver lipids in untreated HFD-fed sham-operated mice: 299.4 ± 59.6 mg/g liver tissue; total liver lipids in telmisartan-treated HFD-fed sham-operated mice: 158.0 ± 31.8 mg/g liver tissue) but did not affect liver lipids in UniNx mice (total liver lipids in untreated HFD-fed UniNx mice: 123.4 ± 17.7 mg/g liver tissue; total liver lipids in telmisartan-treated HFD-fed UniNx mice: 178.5 ± 22.8 mg/g liver tissue) resulting in similar total liver lipids in telmisartan-treated mice of both groups (**Figure 19**).

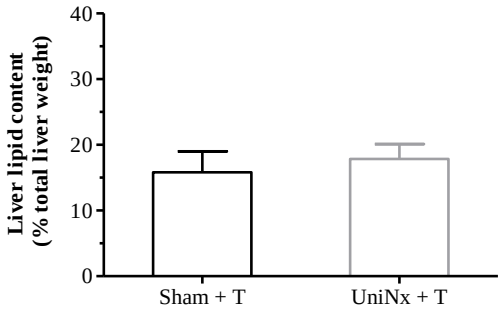

Figure 19 Telmisartan improves hepatic steatosis in HFD-fed sham-operated mice. Total liver lipids were determined and expressed relative to total liver weight in telmisartan-treated HFD-fed sham-operated (black bar) and UniNx mice (grey bar). n=5-6. All error bars represent SEM.

3.12 Similar pro-inflammatory cytokines expression levels in telmisartan-treated HFD-fed sham-operated and UniNx mice

In parallel to improved/decreased hepatic steatosis, mRNA expression levels of pro-inflammatory cytokines in mesenteric adipose tissue were similar between telmisartan-treated HFD-fed sham-operated and UniNx mice. Of note, expression of HIF1α was no longer different between telmisartan-treated sham-operated and UniNx mice (**Figure 20**). These data suggest that telmisartan-treatment improved adipose tissue inflammation in

HFD-fed sham-operated mice since the observed difference in cytokine mRNA expression in untreated mice was no longer present.

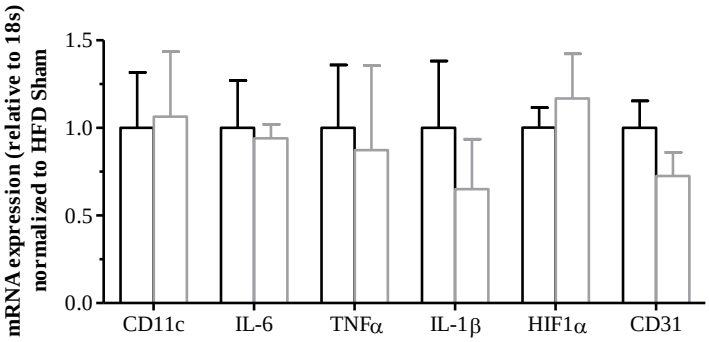

Figure 20 Similar expression of pro-inflammatory cytokines in telmisartan-treated sham-operated and UniNx mice. mRNA expression of respective genes in mesenteric adipose tissue of telmisartan-treated HFD-fed sham-operated (black bars) and UniNx mice (grey bars). n=4-5. Error bars represent SEM. *p < 0.05 and **p < 0.01 (Student's t test).

3.13 No effect of telmisartan-treatment on muscle insulin resistance and capillary rarefaction in HFD-fed UniNx mice

Previously, the angiotensin II receptor blocker losartan was found to reverse insulin resistance through the modulation of muscular circulation in rats with impaired glucose metabolism [157]. We therefore postulated that telmisartan improves muscle insulin sensitivity as well as capillary density in UniNx mice. However, as depicted in **Figure 21A**, 20 weeks of telmisartan-treatment did not improve insulin-stimulated glucose disposal rate (IS-GDR) in UniNx mice (IS-GDR in untreated HFD-fed UniNx mice (**Figure 11B**): 10.6 ± 1.2 mg/kg*min; IS-GDR in telmisartan-treated HFD-fed UniNx mice (**Figure 21A**): 4.2 ± 2.3 mg/kg*min). Accordingly, insulin stimulated glucose uptake was significantly higher in telmisartan-treated HFD-fed sham-operated compared to UniNx mice (**Figure 21B**). Moreover, CD31 expression remained reduced in quadriceps muscle of telmisartan-treated HFD-fed UniNx compared to sham-operated mice (**Figure 21C**). Thus, telmisartan-treatment positively impacts on total body and hepatic insulin sensitivity in HFD-fed sham-

operated mice but does not affect impaired skeletal muscle insulin sensitivity in HFD-fed UniNx mice.

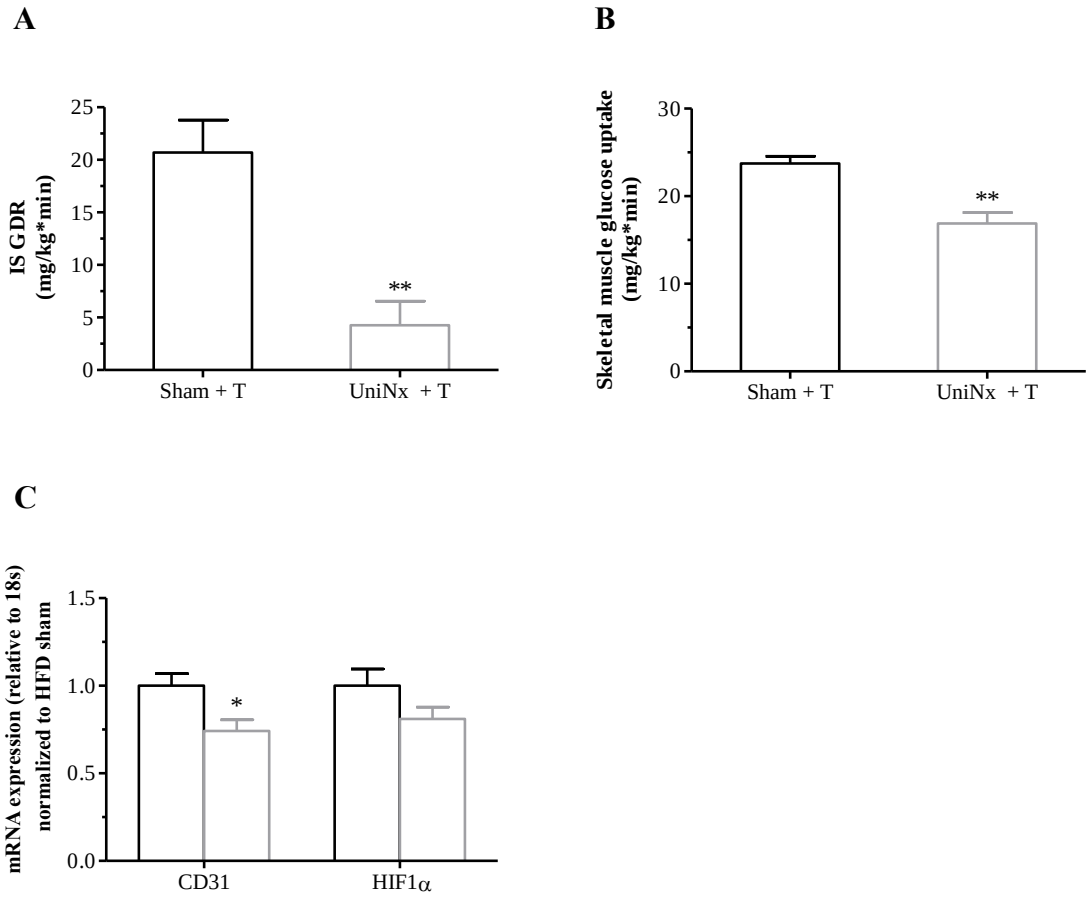

Figure 21 No effect of telmisartan-treatment on muscle insulin resistance and capillary rarefaction in HFD-fed UniNx mice. (**A**) Insulin-stimulated glucose disposal rate (IS GDR) and (**B**) insulin-stimulated glucose uptake into quadriceps muscle during hyperinsulinaemic-euglycaemic clamps (n=4). (**C**) mRNA expression of CD31 and HIF1a in quadriceps muscle of HFD-fed sham-operated (black bars) and UniNx mice (grey bars). n=4-5. Error bars represent SEM. *$p < 0.05$ and **$p < 0.01$ (Student's t test).

4 Discussion

To date, there is increasing evidence that obese patients are more susceptible to the development of progressive renal damage as a consequence of their obesity-related comorbidities, such as T2DM [107]. Conversely, even mild renal dysfunction is thought to increase the risk for developing multiple metabolic derangements, including insulin resistance, an important concern in overweight patients who are already prone to developing T2DM [118, 158]. Although the association between obesity and T2DM are considered established, little is known about their relation to the long-term outcomes in living kidney donor. Several studies have shown that long term consequences of live kidney donation may include a higher propensity of metabolic syndrome, including dyslipidaemia and insulin resistance [100]. Yet, increasing demand for live-donor kidneys has encouraged the use of obese donors despite the evidences that obesity can adversely affect renal function [7]. In view of those observations, we hypothesize that reduced kidney mass which can be induced experimentally in animals by uninephrectomy, may lead to the appearance of all the type 2 diabetes-related traits, as if were, when the animals are challenged in parallel with a HFD. In order to determine whether obese mice were more sensitive to experimental reduced kidney mass, the relation between obesity and uninephrectomy was studied in C57BL/6 mice on long-term outcomes. This was achieved by subjecting lean and obese mice to two experimental protocols: (1) feeding mice on chow or high fat diet after surgical uninephrectomy for up to 20 weeks (2) the treatment of obese mice with the angiotensin II receptor blocker i.e. telmisartan. The specific aim of the project was to test possible mechanism of the RAS activation through which reduced kidney mass may lead to related metabolic disorders by altering the adipose tissue distribution and whole-body glucose homeostasis in diet-induced obese mice.

A potential methodological problem to consider when using contralateral remnant kidney mouse model is whether this model could resemble progressive renal disease, and thus, mimic some clinical aspects of kidney donation in human. It was reported that uninephrectomy leads to progressive kidney dysfunction in rats over a period of time, but it

is not enough to cause CKD progression in C56BL/6 mice [119, 123]. Kidney contributes to whole body metabolism, e.g. to endogenous glucose production [105]. Therefore, a reduction of the functional kidney mass (i.e., a decrease in the number of nephrons), may impact on total body metabolism and homeostasis. On the other hand, as discussed above, diet-induced obesity may also propagate the development of progressive renal disease [110].

Based on the published data of gene expression analysis in mouse kidney samples (same animal samples in our group) by whole genome microarrays in the laboratory of Prof. Gerd Kullak, the impact of HFD on gene expression was stronger than the impact of uninephrectomy. The net effect of uninephrectomy in chow-fed mice was minimal. The studies revealed that the impact of surgical intervention on gene expression between the UniNx-chow/sham-chow groups and the UniNx-HFD/sham-HFD groups were 157 and 136 genes, respectively. In contrast, the impact of HFD was much more significant: 2441 and 2581 gene changes were observed in the groups of sham-HFD versus sham-chow and the groups of UniNx-HFD versus UniNx-chow, respectively. Of note, the combination of UniNx and HFD additionally altered the effects of obesity on gene expression pattern. These data have given us a hint that diet-induced obesity induces metabolic stress and gene expression changes, and these changes were further enhanced by reduced kidney mass. [159, 160].

As shown in **Figure 6A**, the remnant kidneys of UniNx were heavier than sham-operated mice. Nonetheless, removal of 50% of the renal mass was associated with increased cystatin C and creatinine levels in UniNx HFD-fed mice indicating decrease in renal function in these mice (**Figure 8B**). Of note, changes in creatinine levels in HFD-fed UniNx mice were within normal limits (**Figure 8A**). More recently, determination of cystatin C has been proposed to provide a more accurate estimation of the GFR and to be more sensitive in the identification of reduced kidney function than measurement of serum creatinine concentration [161]. Furthermore, it may be a biomarker for potential organ dysfunction in patients with the metabolic syndrome, as it may reflect a response to adipose tissue remodelling and ectopic fat deposition [162]. Thus, the markedly increased cystatin

C levels in HFD-fed UniNx mice may indicate that uninephrectomy has further aggravated HFD-induced metabolic dysfunction.

In order to test the impact of HFD and/or reduced kidney mass on glucose homeostasis, glucose and insulin tolerance was assessed 2, 8, 20 weeks after surgical intervention. As expected, impaired glucose tolerance and insulin resistance developed in HFD-fed mice compared to standard chow-fed mice (**Figure 9**). However, both ipGTT and ipITT were similar in UniNx and sham-operated mice under both standard chow as well as HFD. Using hyperinsulinaemic-euglycaemic clamp, which is considered the gold-standard method to assess insulin sensitivity *in vivo*, total body insulin sensitivity was similar between HFD-fed UniNx and sham-operated mice (**Figure 10**). The beauty of the clamp studies is that insulin sensitivity can be determined in different insulin-sensitive organs. However and surprisingly, uninephrectomised mice were protected from HFD-induced hepatic insulin resistance, but showed deteriorated skeletal muscle resistance (**Figure 11**). This unusual finding of discrepant hepatic and muscle insulin sensitivity begged for the question: what are the potential mechanisms for such discrepancy?

Obesity-associated hepatic insulin sensitivity may be at least partly mediated by adipose tissue inflammation. Particularly, the "portal theory" is claiming that exaggerated release of pro-inflammatory cytokines and/or FFAs from visceral fat directly delivered to the liver via portal vein promotes the development of hepatic insulin resistance (and hepatic steatosis) [23, 163]. Further supporting such notion we found herein reduced visceral adipose tissue inflammation in HFD-fed UniNx mice associated with improved hepatic insulin sensitivity and steatosis (**Figure 12** and **Figure 13A**). Of note, expression of HIF1α was reduced in adipose tissue of HFD-fed UniNx mice (**Figure 13A**). Selective inhibition of HIF1α was previously reported to reduce adipose tissue inflammation as well as hepatic steatosis in HFD-fed mice [19]. Conversely, overexpression of HIF1α induced adipose tissue fibrosis and inflammation as well as hepatic steatosis [20]. Thus, uninephrectomy is associated with decreased HIF1a expression in adipose tissue and thereby may contribute to reduced adipose inflammation; and consequently preserved

hepatic insulin sensitivity. Such notion is further supported by the fact that treatment with telmisartan abolished differences in mRNA expression of HIF1α as well as pro-inflammatory cytokines and improved hepatic insulin sensitivity in sham-operated mice (**Figure 20**). Currently, it remains to be elucidated how uninephrectomy regulates/ modulates HIF1α expression in adipose tissue.

However, improved hepatic insulin sensitivity may be independent of adipose tissue inflammation. Intriguingly, unpublished findings in the laboratory of Prof. Gerd Kullak have recently described a two fold increase in bile acid levels in UniNx mice. Bile acids were recently reported to activate the farnesoid X receptor (FXR) and thereby reversing HFD-induced hepatic insulin resistance and improving hepatic steatosis [164]. Moreover, recent clinical studies have suggested that FXR activation appears to improve insulin resistance and fatty liver status in patients with T2DM [165]. Herein, we found a trend towards increased bile acid levels in HFD-fed UniNx compared to sham-operated mice, although such difference did not reach statistical significance (**Table 1**). Thus, increased circulating bile acid levels may have at least partly contributed to improved hepatic insulin sensitivity and steatosis in HFD-fed UniNx mice.

In contrast to improved hepatic insulin sensitivity, skeletal muscle insulin sensitivity was further deteriorated in HFD-fed UniNx mice. The precise mechanism how UniNx may negatively impact on skeletal muscle insulin sensitivity remains unclear. The observed discrepancy of preserved muscle insulin sensitivity *ex vivo* but deteriorated muscle insulin resistance *in vivo* indicated impaired insulin delivery to the sarcolemma in UniNx mice. It was previously reported that insulin increases microvascular blood flow to the muscle contributing to approximately half of the insulin-mediated glucose uptake [78]. Accordingly, muscle capillary density strongly correlates with peripheral insulin action [166]. Conversely, capillary rarefaction was associated with insulin resistance both in humans and rodents [79, 83, 84]. Thus, UniNx may propagate capillary rarefaction of skeletal muscle. Indeed, mRNA expression and histological staining of CD31 were decreased pointing towards reduced capillary density in skeletal muscle of HFD-fed UniNx mice (**Figure 15**). Our results are in accordance with Flinsinski et al, who reported

reduced numbers of capillaries as well as a decreased capillary-to-fiber ratio in gastrocnemius and longissimus muscle in UniNx male Wistar rats [167]. Of note, treatment with the angiotensin II receptor blocker telmisartan had no impact on capillary density in UniNx mice suggesting that UniNx-associated capillary rarefaction is not dependent on activation of the RAS whereas it may modulate muscular circulation and thereby insulin sensitivity as was previously reported for the angiotensin II receptor blocker losartan in rats [84]. Potentially, reduced muscle capillary density may relate to decreased HIF1a mRNA expression in skeletal muscle of UniNx mice. HIF1α is the master regulator of transcriptional responses to hypoxia and a transcriptional activator of gene encoding vascular endothelial growth factor (VEGF) and other important mediators of angiogenesis [80]. Importantly, UniNx and subtotal nephrectomy in Wistar rats were associated with reduced expression of HIF1α, VEGF A and VEGF receptor in gastrocnemius muscle [168]. Moreover, muscle-specific deletion of VEGF resulted in capillary rarefaction and diminished insulin-induced muscle glucose uptake *in vivo* independent of defects in insulin action at the myocyte [83]. Thus, reduced expression of HIF1α may be causally linked to reduced capillary density observed in skeletal muscle of UniNx mice.

There is evidence activation of the RAS/angiotensin receptors (ATRs) impairs insulin signalling in adipose tissue, skeletal muscle, and liver by inducing oxidative stress and/or activating serine kinases such as NFκB and ERK1/2 leading to impaired insulin signalling [169]. Overnutrition may activate the RAS, and thus may contribute to the pathogenesis of insulin resistance, particularly in the presence of reduced renal function [39, 107]. Thus, we hypothesized that the observed deterioration of muscle insulin sensitivity in UniNx mice was due, at least partly, to activation of the RAS. Indeed, we found indirect evidence for activation of the RAS in UniNx mice as demonstrated by increased angiotensin I levels 2, 8, 20 weeks after surgery (**Figure 16**).

However, treatment with the angiotensin II type I receptor blocker telmisartan did not improve skeletal muscle insulin sensitivity and had no impact on capillary density in UniNx mice, suggesting that UniNx-associated capillary rarefaction is not dependent on

activation of the RAS whereas it may modulate muscular circulation and thereby insulin sensitivity, as was previously reported for the angiotensin II receptor blocker losartan in rats [84]. In contrast, telmisartan-treatment improved glucose tolerance in HFD-fed sham-operated mice, probably via reduction of adipose tissue inflammation, and consequently preservation of hepatic insulin sensitivity [40, 170]. Accordingly, treatment with telmisartan abolished differences in mRNA expression of HIF1α as well as pro-inflammatory cytokines between UniNx and sham-operated mice and improved hepatic insulin sensitivity in the latter. Of note, lacking effect of telmisartan-treatment on insulin resistance and increased circulating angiotensin I levels in HFD-fed UniNx mice may be explained by the development of angiotensin II resistance in these mice.

In conclusion, UniNx unexpectedly protects HFD-fed mice from obesity-induced adipose tissue inflammation and hepatic insulin resistance potentially via a reduction in HIF1α expression. In contrast, UniNx leads to capillary rarefaction in skeletal muscle and, thus, deteriorates HFD-induced skeletal muscle glucose disposal *in vivo*.

5 References

1. WHO, *Obesity and overweight. Fact sheet number 311 http://www.who.int/mediacentre/factsheets/fs311/en/.* 2006.
2. Ng, M., et al., *Global, regional, and national prevalence of overweight and obesity in children and adults during 1980–2013: a systematic analysis for the Global Burden of Disease Study 2013.* The Lancet, (0).
3. Lim, S.S., et al., *A comparative risk assessment of burden of disease and injury attributable to 67 risk factors and risk factor clusters in 21 regions, 1990?2010: a systematic analysis for the Global Burden of Disease Study 2010.* The Lancet, 2012. **380**(9859): p. 2224-2260.
4. The diabetes pandemic, L., *The diabetes pandemic.* The Lancet, 2011. **378**(9786): p. 99.
5. KDOQI, G.N. *http://www.kidney.org/professionals/kdoqi/guideline_diabetes/background.htm*.
6. Friedman, A.N., et al., *Demographics and trends in overweight and obesity in patients at time of kidney transplantation.* Am J Kidney Dis, 2003. **41**(2): p. 480-7.
7. Tavakol, M.M., et al., *Long-term renal function and cardiovascular disease risk in obese kidney donors.* Clin J Am Soc Nephrol, 2009. **4**(7): p. 1230-8.
8. Weisberg, S.P., et al., *Obesity is associated with macrophage accumulation in adipose tissue.* Journal of Clinical Investigation, 2003. **112**(12): p. 1796-1808.
9. Kershaw, E.E. and J.S. Flier, *Adipose tissue as an endocrine organ.* J Clin Endocrinol Metab, 2004. **89**(6): p. 2548-56.
10. Ouchi, N., et al., *Adipokines in inflammation and metabolic disease.* Nat Rev Immunol, 2011. **11**(2): p. 85-97.
11. Lumeng, C.N., J.L. Bodzin, and A.R. Saltiel, *Obesity induces a phenotypic switch in adipose tissue macrophage polarization.* J Clin Invest, 2007. **117**(1): p. 175-84.
12. Schenk, S., M. Saberi, and J.M. Olefsky, *Insulin sensitivity: modulation by nutrients and inflammation.* J Clin Invest, 2008. **118**(9): p. 2992-3002.
13. Rotter, V., I. Nagaev, and U. Smith, *Interleukin-6 (IL-6) induces insulin resistance in 3T3-L1 adipocytes and is, like IL-8 and tumor necrosis factor-alpha, overexpressed in human fat cells from insulin-resistant subjects.* J Biol Chem, 2003. **278**(46): p. 45777-84.
14. Kim, H.J., et al., *Differential effects of interleukin-6 and -10 on skeletal muscle and liver insulin action in vivo.* Diabetes, 2004. **53**(4): p. 1060-7.
15. Souza, S.C., et al., *Overexpression of perilipin A and B blocks the ability of tumor necrosis factor alpha to increase lipolysis in 3T3-L1 adipocytes.* J Biol Chem, 1998. **273**(38): p. 24665-9.
16. Gustafson, B. and U. Smith, *Cytokines promote Wnt signaling and inflammation and impair the normal differentiation and lipid accumulation in 3T3-L1 preadipocytes.* J Biol Chem, 2006. **281**(14): p. 9507-16.

17. Ye, J., *Adipose tissue vascularization: its role in chronic inflammation.* Curr Diab Rep, 2011. **11**(3): p. 203-10.
18. Semenza, G.L., *HIF-1: mediator of physiological and pathophysiological responses to hypoxia.* J Appl Physiol (1985), 2000. **88**(4): p. 1474-80.
19. Sun, K., et al., *Selective inhibition of hypoxia-inducible factor 1alpha ameliorates adipose tissue dysfunction.* Mol Cell Biol, 2013. **33**(5): p. 904-17.
20. Halberg, N., et al., *Hypoxia-inducible factor 1alpha induces fibrosis and insulin resistance in white adipose tissue.* Mol Cell Biol, 2009. **29**(16): p. 4467-83.
21. Bruun, J.M., et al., *Higher production of IL-8 in visceral vs. subcutaneous adipose tissue. Implication of nonadipose cells in adipose tissue.* Am J Physiol Endocrinol Metab, 2004. **286**(1): p. E8-13.
22. Krysiak, R., K. Labuzek, and B. Okopien, *Effect of atorvastatin and fenofibric acid on adipokine release from visceral and subcutaneous adipose tissue of patients with mixed dyslipidemia and normolipidemic subjects.* Pharmacol Rep, 2009. **61**(6): p. 1134-45.
23. Item, F. and D. Konrad, *Visceral fat and metabolic inflammation: the portal theory revisited.* Obes Rev, 2012. **13 Suppl 2**: p. 30-9.
24. Despres, J.P. and I. Lemieux, *Abdominal obesity and metabolic syndrome.* Nature, 2006. **444**(7121): p. 881-7.
25. Tan, C.Y. and A. Vidal-Puig, *Adipose tissue expandability: the metabolic problems of obesity may arise from the inability to become more obese.* Biochem Soc Trans, 2008. **36**(Pt 5): p. 935-40.
26. McQuaid, S.E., et al., *Downregulation of adipose tissue fatty acid trafficking in obesity: a driver for ectopic fat deposition?* Diabetes, 2011. **60**(1): p. 47-55.
27. Jacob, S., et al., *Association of increased intramyocellular lipid content with insulin resistance in lean nondiabetic offspring of type 2 diabetic subjects.* Diabetes, 1999. **48**(5): p. 1113-9.
28. Moro, C., S. Bajpeyi, and S.R. Smith, *Determinants of intramyocellular triglyceride turnover: implications for insulin sensitivity.* Am J Physiol Endocrinol Metab, 2008. **294**(2): p. E203-13.
29. Hegele, R.A., et al., *Thematic review series: Adipocyte Biology. Lipodystrophies: windows on adipose biology and metabolism.* J Lipid Res, 2007. **48**(7): p. 1433-44.
30. Goodfriend, T.L., M.E. Elliott, and K.J. Catt, *Angiotensin receptors and their antagonists.* N Engl J Med, 1996. **334**(25): p. 1649-54.
31. Matsusaka, T. and I. Ichikawa, *Biological functions of angiotensin and its receptors.* Annu Rev Physiol, 1997. **59**: p. 395-412.
32. Kalupahana, N.S. and N. Moustaid-Moussa, *The renin-angiotensin system: a link between obesity, inflammation and insulin resistance.* Obes Rev, 2012. **13**(2): p. 136-49.
33. Jones, B.H., et al., *Angiotensinogen gene expression in adipose tissue: analysis of obese models and hormonal and nutritional control.* Am J Physiol, 1997. **273**(1 Pt 2): p. R236-42.
34. Paul, M., A. Poyan Mehr, and R. Kreutz, *Physiology of local renin-angiotensin systems.* Physiol Rev, 2006. **86**(3): p. 747-803.

35. Cassis, L.A., et al., *Local adipose tissue renin-angiotensin system.* Curr Hypertens Rep, 2008. **10**(2): p. 93-8.
36. Marcus, Y., G. Shefer, and N. Stern, *Adipose tissue renin-angiotensin-aldosterone system (RAAS) and progression of insulin resistance.* Mol Cell Endocrinol, 2013. **378**(1-2): p. 1-14.
37. Kouyama, R., et al., *Attenuation of diet-induced weight gain and adiposity through increased energy expenditure in mice lacking angiotensin II type 1a receptor.* Endocrinology, 2005. **146**(8): p. 3481-9.
38. Lee, M.H., et al., *Angiotensin receptor blockers improve insulin resistance in type 2 diabetic rats by modulating adipose tissue.* Kidney Int, 2008. **74**(7): p. 890-900.
39. Yvan-Charvet, L. and A. Quignard-Boulange, *Role of adipose tissue renin-angiotensin system in metabolic and inflammatory diseases associated with obesity*. Kidney Int, 2011. **79**(2): p. 162-8.
40. Foryst-Ludwig, A., et al., *PPARgamma activation attenuates T-lymphocyte-dependent inflammation of adipose tissue and development of insulin resistance in obese mice.* Cardiovasc Diabetol, 2010. **9**: p. 64.
41. Zhao, Z.Q., et al., *Angiotensin II receptor blocker telmisartan prevents new-onset diabetes in pre-diabetes OLETF rats on a high-fat diet: evidence of anti-diabetes action.* Can J Diabetes, 2013. **37**(3): p. 156-68.
42. Hartono, S.P., et al., *Combined effect of hyperfiltration and renin angiotensin system activation on development of chronic kidney disease in diabetic db/db mice.* BMC Nephrol, 2014. **15**: p. 58.
43. Sui, Y., et al., *Pancreatic islet beta-cell deficit and glucose intolerance in rats with uninephrectomy.* Cell Mol Life Sci, 2007. **64**(23): p. 3119-28.
44. Zhao, H.L., et al., *Fat redistribution and adipocyte transformation in uninephrectomized rats.* Kidney Int, 2008. **74**(4): p. 467-77.
45. Groop, L.C., *Insulin resistance: the fundamental trigger of type 2 diabetes.* Diabetes Obes Metab, 1999. **1 Suppl 1**: p. S1-7.
46. Pham, H., K.M. Utzschneider, and I.H. de Boer, *Measurement of insulin resistance in chronic kidney disease.* Curr Opin Nephrol Hypertens, 2011. **20**(6): p. 640-6.
47. Reaven, G.M., *The insulin resistance syndrome: definition and dietary approaches to treatment.* Annu Rev Nutr, 2005. **25**: p. 391-406.
48. Steinbeck, K.S., *Insulin resistance syndrome in children and adolescents: clinical meaning and indication for action.* Int J Obes Relat Metab Disord, 0000. **28**(7): p. 829-832.
49. Tam, C.S., et al., *Defining insulin resistance from hyperinsulinemic-euglycemic clamps.* Diabetes Care, 2012. **35**(7): p. 1605-10.
50. Taniguchi, C.M., B. Emanuelli, and C.R. Kahn, *Critical nodes in signalling pathways: insights into insulin action.* Nat Rev Mol Cell Biol, 2006. **7**(2): p. 85-96.
51. White, M.F., *Insulin signaling in health and disease.* Science, 2003. **302**(5651): p. 1710-1.
52. Kahn, C.R., *Banting Lecture. Insulin action, diabetogenes, and the cause of type II diabetes.* Diabetes, 1994. **43**(8): p. 1066-84.

53. Li, T., et al., *Glucose and insulin induction of bile acid synthesis: mechanisms and implication in diabetes and obesity.* J Biol Chem, 2012. **287**(3): p. 1861-73.
54. Butler, A.A., et al., *Insulin-like growth factor-I receptor signal transduction: at the interface between physiology and cell biology.* Comp Biochem Physiol B Biochem Mol Biol, 1998. **121**(1): p. 19-26.
55. Reaven, G.M., *Role of Insulin Resistance in Human Disease.* Diabetes, 1988. **37**(12): p. 1595-1607.
56. Konner, A.C. and J.C. Bruning, *Selective insulin and leptin resistance in metabolic disorders.* Cell Metab, 2012. **16**(2): p. 144-52.
57. Smith, U., *Impaired ('diabetic') insulin signaling and action occur in fat cells long before glucose intolerance--is insulin resistance initiated in the adipose tissue?* Int J Obes Relat Metab Disord, 2002. **26**(7): p. 897-904.
58. Sun, X.J., et al., *Structure of the insulin receptor substrate IRS-1 defines a unique signal transduction protein.* Nature, 1991. **352**(6330): p. 73-7.
59. Biddinger, S.B. and C.R. Kahn, *From mice to men: insights into the insulin resistance syndromes.* Annu Rev Physiol, 2006. **68**: p. 123-58.
60. Engelman, J.A., J. Luo, and L.C. Cantley, *The evolution of phosphatidylinositol 3-kinases as regulators of growth and metabolism.* Nat Rev Genet, 2006. **7**(8): p. 606-619.
61. Bryant, N.J., R. Govers, and D.E. James, *Regulated transport of the glucose transporter GLUT4.* Nat Rev Mol Cell Biol, 2002. **3**(4): p. 267-277.
62. Michell, B.J., et al., *The Akt kinase signals directly to endothelial nitric oxide synthase.* Current Biology, 1999. **9**(15): p. 845-S1.
63. Margolis, B. and E.Y. Skolnik, *Activation of Ras by receptor tyrosine kinases.* J Am Soc Nephrol, 1994. **5**(6): p. 1288-99.
64. Avruch, J., *Insulin signal transduction through protein kinase cascades.* Mol Cell Biochem, 1998. **182**(1-2): p. 31-48.
65. Pessin, J.E. and A.R. Saltiel, *Signaling pathways in insulin action: molecular targets of insulin resistance.* J Clin Invest, 2000. **106**(2): p. 165-9.
66. Guilherme, A., et al., *Adipocyte dysfunctions linking obesity to insulin resistance and type 2 diabetes.* Nat Rev Mol Cell Biol, 2008. **9**(5): p. 367-77.
67. Rubio-Cabezas, O., et al., *Partial lipodystrophy and insulin resistant diabetes in a patient with a homozygous nonsense mutation in CIDEC.* EMBO Mol Med, 2009. **1**(5): p. 280-7.
68. Cortes, V.A., et al., *Leptin ameliorates insulin resistance and hepatic steatosis in Agpat2-/- lipodystrophic mice independent of hepatocyte leptin receptors.* J Lipid Res, 2014. **55**(2): p. 276-88.
69. Bagby, S.P., *Obesity-initiated metabolic syndrome and the kidney: a recipe for chronic kidney disease?* J Am Soc Nephrol, 2004. **15**(11): p. 2775-91.
70. Zhao, H.L., et al., *Lipid partitioning after uninephrectomy.* Acta Diabetol, 2011. **48**(4): p. 317-28.
71. Samuel, V.T., K.F. Petersen, and G.I. Shulman, *Lipid-induced insulin resistance: unravelling the mechanism.* Lancet, 2010. **375**(9733): p. 2267-77.

72. Perry, R.J., et al., *The role of hepatic lipids in hepatic insulin resistance and type 2 diabetes.* Nature, 2014. **510**(7503): p. 84-91.
73. Miyazaki, Y., et al., *Abdominal fat distribution and peripheral and hepatic insulin resistance in type 2 diabetes mellitus.* Am J Physiol Endocrinol Metab, 2002. **283**(6): p. E1135-43.
74. Suganami, T., M. Tanaka, and Y. Ogawa, *Adipose tissue inflammation and ectopic lipid accumulation.* Endocr J, 2012. **59**(10): p. 849-57.
75. Ferrannini, E., et al., *The disposal of an oral glucose load in patients with non-insulin-dependent diabetes.* Metabolism, 1988. **37**(1): p. 79-85.
76. Petersen, K.F. and G.I. Shulman, *Cellular mechanism of insulin resistance in skeletal muscle.* J R Soc Med, 2002. **95 Suppl 42**: p. 8-13.
77. Schmitz-Peiffer, C., *Signalling aspects of insulin resistance in skeletal muscle: mechanisms induced by lipid oversupply.* Cell Signal, 2000. **12**(9-10): p. 583-94.
78. Rattigan, S., M.G. Clark, and E.J. Barrett, *Acute vasoconstriction-induced insulin resistance in rat muscle in vivo.* Diabetes, 1999. **48**(3): p. 564-9.
79. Gavin, T.P., et al., *Lower capillary density but no difference in VEGF expression in obese vs. lean young skeletal muscle in humans.* J Appl Physiol (1985), 2005. **98**(1): p. 315-21.
80. Semenza, G.L., *Angiogenesis in ischemic and neoplastic disorders.* Annu Rev Med, 2003. **54**: p. 17-28.
81. Halseth, A.E., D.P. Bracy, and D.H. Wasserman, *Limitations to basal and insulin-stimulated skeletal muscle glucose uptake in the high-fat-fed rat.* Am J Physiol Endocrinol Metab, 2000. **279**(5): p. E1064-71.
82. Chiu, J.D., et al., *Direct administration of insulin into skeletal muscle reveals that the transport of insulin across the capillary endothelium limits the time course of insulin to activate glucose disposal.* Diabetes, 2008. **57**(4): p. 828-35.
83. Bonner, J.S., et al., *Muscle-specific vascular endothelial growth factor deletion induces muscle capillary rarefaction creating muscle insulin resistance.* Diabetes, 2013. **62**(2): p. 572-80.
84. Guo, Q., et al., *Losartan modulates muscular capillary density and reverses thiazide diuretic-exacerbated insulin resistance in fructose-fed rats.* Hypertens Res, 2012. **35**(1): p. 48-54.
85. Wild, S., et al., *Global prevalence of diabetes: estimates for the year 2000 and projections for 2030.* Diabetes Care, 2004. **27**(5): p. 1047-53.
86. Whiting, D.R., et al., *IDF diabetes atlas: global estimates of the prevalence of diabetes for 2011 and 2030.* Diabetes Res Clin Pract, 2011. **94**(3): p. 311-21.
87. Colditz, G.A., et al., *Weight gain as a risk factor for clinical diabetes mellitus in women.* Ann Intern Med, 1995. **122**(7): p. 481-6.
88. Chan, J.M., et al., *Obesity, fat distribution, and weight gain as risk factors for clinical diabetes in men.* Diabetes Care, 1994. **17**(9): p. 961-9.
89. Kahn, S.E., R.L. Hull, and K.M. Utzschneider, *Mechanisms linking obesity to insulin resistance and type 2 diabetes.* Nature, 2006. **444**(7121): p. 840-6.
90. Ehses, J.A., et al., *Increased number of islet-associated macrophages in type 2 diabetes.* Diabetes, 2007. **56**(9): p. 2356-70.

91. Boni-Schnetzler, M., et al., *Increased interleukin (IL)-1beta messenger ribonucleic acid expression in beta -cells of individuals with type 2 diabetes and regulation of IL-1beta in human islets by glucose and autostimulation.* J Clin Endocrinol Metab, 2008. **93**(10): p. 4065-74.
92. Welsh, N., et al., *Is there a role for locally produced interleukin-1 in the deleterious effects of high glucose or the type 2 diabetes milieu to human pancreatic islets?* Diabetes, 2005. **54**(11): p. 3238-44.
93. Smith-Palmer, J., et al., *Assessment of the association between glycemic variability and diabetes-related complications in type 1 and type 2 diabetes.* Diabetes Res Clin Pract, 2014.
94. Cade, W.T., *Diabetes-related microvascular and macrovascular diseases in the physical therapy setting.* Phys Ther, 2008. **88**(11): p. 1322-35.
95. Deshpande, A.D., M. Harris-Hayes, and M. Schootman, *Epidemiology of diabetes and diabetes-related complications.* Phys Ther, 2008. **88**(11): p. 1254-64.
96. Parving, H.H., et al., *Evolving strategies for renoprotection: diabetic nephropathy.* Curr Opin Nephrol Hypertens, 2001. **10**(4): p. 515-22.
97. Giri, M., *Choice of renal replacement therapy in patients with diabetic end stage renal disease.* EDTNA ERCA J, 2004. **30**(3): p. 138-42.
98. Keane, W.F., et al., *The risk of developing end-stage renal disease in patients with type 2 diabetes and nephropathy: the RENAAL study.* Kidney Int, 2003. **63**(4): p. 1499-507.
99. Friedman, E.A., A.L. Friedman, and P. Eggers, *End-stage renal disease in diabetic persons: is the pandemic subsiding?* Kidney Int Suppl, 2006(104): p. S51-4.
100. Ferreira-Filho, S.R., L. da Silva Passos, and M.B. Ribeiro, *Corporeal weight gain and metabolic syndrome in living kidney donors after nephrectomy.* Transplant Proc, 2007. **39**(2): p. 403-6.
101. Ibrahim, H.N., et al., *Diabetes after kidney donation.* Am J Transplant, 2010. **10**(2): p. 331-7.
102. Bobulescu, I.A. and O.W. Moe, *Na+/H+ exchangers in renal regulation of acid-base balance.* Semin Nephrol, 2006. **26**(5): p. 334-44.
103. DeFronzo, R.A., J.A. Davidson, and S. Del Prato, *The role of the kidneys in glucose homeostasis: a new path towards normalizing glycaemia.* Diabetes Obes Metab, 2012. **14**(1): p. 5-14.
104. Mather, A. and C. Pollock, *Glucose handling by the kidney.* Kidney Int Suppl, 2011(120): p. S1-6.
105. Gerich, J.E., *Role of the kidney in normal glucose homeostasis and in the hyperglycaemia of diabetes mellitus: therapeutic implications.* Diabet Med, 2010. **27**(2): p. 136-42.
106. National Kidney, F., *K/DOQI clinical practice guidelines for chronic kidney disease: evaluation, classification, and stratification.* Am J Kidney Dis, 2002. **39**(2 Suppl 1): p. S1-266.
107. Hall, J.E., et al., *Is obesity a major cause of chronic kidney disease?* Adv Ren Replace Ther, 2004. **11**(1): p. 41-54.

108. Yokoyama, H., et al., *Determinants of decline in glomerular filtration rate in nonproteinuric subjects with or without diabetes and hypertension.* Clin J Am Soc Nephrol, 2009. **4**(9): p. 1432-40.
109. Seliger, S.L., *Inflammation and dyslipidemia in nephropathy: an epidemiologic perspective.* Kidney Int, 2006. **69**(2): p. 206-8.
110. de Jong, P.E., et al., *Obesity and target organ damage: the kidney.* Int J Obes Relat Metab Disord, 2002. **26 Suppl 4**: p. S21-4.
111. Kasiske, B.L. and J.T. Crosson, *Renal disease in patients with massive obesity.* Arch Intern Med, 1986. **146**(6): p. 1105-9.
112. Cohen, A.H., *Massive obesity and the kidney. A morphologic and statistical study.* Am J Pathol, 1975. **81**(1): p. 117-30.
113. Kambham, N., et al., *Obesity-related glomerulopathy: an emerging epidemic.* Kidney Int, 2001. **59**(4): p. 1498-509.
114. Patel, S.S., P.L. Kimmel, and A. Singh, *New clinical practice guidelines for chronic kidney disease: a framework for K/DOQI.* Semin Nephrol, 2002. **22**(6): p. 449-58.
115. Molitch, M.E., et al., *Nephropathy in diabetes.* Diabetes Care, 2004. **27 Suppl 1**: p. S79-83.
116. DeFronzo, R.A., et al., *Insulin resistance in uremia.* J Clin Invest, 1981. **67**(2): p. 563-8.
117. Mak, R.H., G.B. Haycock, and C. Chantler, *Glucose intolerance in children with chronic renal failure.* Kidney Int Suppl, 1983. **15**: p. S22-6.
118. Shehab-Eldin, W., et al., *Susceptibility to insulin resistance after kidney donation: a pilot observational study.* Am J Nephrol, 2009. **30**(4): p. 371-6.
119. Hayslett, J.P., *Functional adaptation to reduction in renal mass.* Physiol Rev, 1979. **59**(1): p. 137-64.
120. Kren, S. and T.H. Hostetter, *The course of the remnant kidney model in mice.* Kidney Int, 1999. **56**(1): p. 333-7.
121. Hostetter, T.H., et al., *Hyperfiltration in remnant nephrons: a potentially adverse response to renal ablation.* Am J Physiol, 1981. **241**(1): p. F85-93.
122. Orsic, V., et al., *Impaired kidney function in rats six months after unilateral nephrectomy - an old story, a new perspective.* Med Glas (Zenica), 2011. **8**(2): p. 185-91.
123. Fogo, A.B., *Animal models of FSGS: lessons for pathogenesis and treatment.* Semin Nephrol, 2003. **23**(2): p. 161-71.
124. Leelahavanichkul, A., et al., *Angiotensin II overcomes strain-dependent resistance of rapid CKD progression in a new remnant kidney mouse model.* Kidney Int, 2010. **78**(11): p. 1136-53.
125. Hsu, C.Y., et al., *Body mass index and risk for end-stage renal disease.* Ann Intern Med, 2006. **144**(1): p. 21-8.
126. Wang, Y., et al., *Association between obesity and kidney disease: a systematic review and meta-analysis.* Kidney Int, 2008. **73**(1): p. 19-33.
127. Sun, L., et al., *Role of sterol regulatory element-binding protein 1 in regulation of renal lipid metabolism and glomerulosclerosis in diabetes mellitus.* J Biol Chem, 2002. **277**(21): p. 18919-27.

128. Jiang, T., et al., *Diet-induced obesity in C57BL/6J mice causes increased renal lipid accumulation and glomerulosclerosis via a sterol regulatory element-binding protein-1c-dependent pathway.* J Biol Chem, 2005. **280**(37): p. 32317-25.
129. Knight, S.F. and J.D. Imig, *Obesity, insulin resistance, and renal function.* Microcirculation, 2007. **14**(4-5): p. 349-62.
130. Ix, J.H. and K. Sharma, *Mechanisms linking obesity, chronic kidney disease, and fatty liver disease: the roles of fetuin-A, adiponectin, and AMPK.* J Am Soc Nephrol, 2010. **21**(3): p. 406-12.
131. Orlic, L., et al., *Chronic kidney disease and nonalcoholic Fatty liver disease-is there a link?* Gastroenterol Res Pract, 2014. **2014**: p. 847539.
132. Targher, G., et al., *Risk of chronic kidney disease in patients with non-alcoholic fatty liver disease: is there a link?* J Hepatol, 2011. **54**(5): p. 1020-9.
133. Yilmaz, Y., et al., *Microalbuminuria in nondiabetic patients with nonalcoholic fatty liver disease: association with liver fibrosis.* Metabolism, 2010. **59**(9): p. 1327-30.
134. Munshi, M.K., M.N. Uddin, and S.S. Glaser, *The role of the renin-angiotensin system in liver fibrosis.* Exp Biol Med (Maywood), 2011. **236**(5): p. 557-66.
135. Sakkas, G.K., et al., *Atrophy of non-locomotor muscle in patients with end-stage renal failure.* Nephrol Dial Transplant, 2003. **18**(10): p. 2074-81.
136. Workeneh, B.T. and W.E. Mitch, *Review of muscle wasting associated with chronic kidney disease.* Am J Clin Nutr, 2010. **91**(4): p. 1128S-1132S.
137. Brink, M., et al., *Angiotensin II induces skeletal muscle wasting through enhanced protein degradation and down-regulates autocrine insulin-like growth factor I.* Endocrinology, 2001. **142**(4): p. 1489-96.
138. Price, S.R., et al., *Muscle atrophy in chronic kidney disease results from abnormalities in insulin signaling.* J Ren Nutr, 2010. **20**(5 Suppl): p. S24-8.
139. Rajan, V.R. and W.E. Mitch, *Muscle wasting in chronic kidney disease: the role of the ubiquitin proteasome system and its clinical impact.* Pediatr Nephrol, 2008. **23**(4): p. 527-35.
140. Bailey, J.L., *Insulin resistance and muscle metabolism in chronic kidney disease.* ISRN Endocrinol, 2013. **2013**: p. 329606.
141. Wolf, G., U. Butzmann, and U.O. Wenzel, *The renin-angiotensin system and progression of renal disease: from hemodynamics to cell biology.* Nephron Physiol, 2003. **93**(1): p. P3-13.
142. Itani, S.I., et al., *Involvement of protein kinase C in human skeletal muscle insulin resistance and obesity.* Diabetes, 2000. **49**(8): p. 1353-8.
143. Russell, A.P., *Lipotoxicity: the obese and endurance-trained paradox.* Int J Obes Relat Metab Disord, 2004. **28 Suppl 4**: p. S66-71.
144. Konrad, D., A. Rudich, and E.J. Schoenle, *Improved glucose tolerance in mice receiving intraperitoneal transplantation of normal fat tissue.* Diabetologia, 2007. **50**(4): p. 833-9.
145. Rytka, J.M., et al., *The portal theory supported by venous drainage-selective fat transplantation.* Diabetes, 2011. **60**(1): p. 56-63.

146. Fisher, S.J. and C.R. Kahn, *Insulin signaling is required for insulin's direct and indirect action on hepatic glucose production.* The Journal of clinical investigation, 2003. **111**(4): p. 463-8.
147. Kim, J.K., et al., *Redistribution of substrates to adipose tissue promotes obesity in mice with selective insulin resistance in muscle.* The Journal of clinical investigation, 2000. **105**(12): p. 1791-7.
148. Saberi, M., et al., *Novel liver-specific TORC2 siRNA corrects hyperglycemia in rodent models of type 2 diabetes.* American journal of physiology. Endocrinology and metabolism, 2009. **297**(5): p. E1137-E1146.
149. Bruce, C.R., et al., *Overexpression of sphingosine kinase 1 prevents ceramide accumulation and ameliorates muscle insulin resistance in high-fat diet-fed mice.* Diabetes, 2012. **61**(12): p. 3148-55.
150. Wueest, S., et al., *Fas (CD95) expression in myeloid cells promotes obesity-induced muscle insulin resistance.* EMBO Mol Med, 2014. **6**(1): p. 43-56.
151. Knight, J.A., S. Anderson, and J.M. Rawle, *Chemical basis of the sulfo-phospho-vanillin reaction for estimating total serum lipids.* Clin Chem, 1972. **18**(3): p. 199-202.
152. Hansen, P.A., E.A. Gulve, and J.O. Holloszy, *Suitability of 2-deoxyglucose for in vitro measurement of glucose transport activity in skeletal muscle.* Journal of applied physiology, 1994. **76**(2): p. 979-85.
153. Wueest, S., et al., *Deletion of Fas in adipocytes relieves adipose tissue inflammation and hepatic manifestations of obesity in mice.* J Clin Invest, 2010. **120**(1): p. 191-202.
154. Diamond-Stanic, M.K. and E.J. Henriksen, *Direct inhibition by angiotensin II of insulin-dependent glucose transport activity in mammalian skeletal muscle involves a ROS-dependent mechanism.* Arch Physiol Biochem, 2010. **116**(2): p. 88-95.
155. Henriksen, E.J. and M. Prasannarong, *The role of the renin-angiotensin system in the development of insulin resistance in skeletal muscle.* Mol Cell Endocrinol, 2013. **378**(1-2): p. 15-22.
156. Wei, Y., et al., *Angiotensin II-induced skeletal muscle insulin resistance mediated by NF-kappaB activation via NADPH oxidase.* Am J Physiol Endocrinol Metab, 2008. **294**(2): p. E345-51.
157. Guo, Q., et al., *Losartan modulates muscular capillary density and reverses thiazide diuretic-exacerbated insulin resistance in fructose-fed rats.* Hypertension research : official journal of the Japanese Society of Hypertension, 2012. **35**(1): p. 48-54.
158. Nerpin, E., et al., *Insulin sensitivity measured with euglycemic clamp is independently associated with glomerular filtration rate in a community-based cohort.* Diabetes Care, 2008. **31**(8): p. 1550-5.
159. Gai, Z., et al., *Uninephrectomy augments the effects of high fat diet induced obesity on gene expression in mouse kidney.* Biochim Biophys Acta, 2014.
160. Gai, Z., *Genome-wide profiling to analyze the effects of high fat diet induced obesity on renal gene expression in mouse with reduced renal mass.* Genomics Data, 2014. **2**(0): p. 42-43.

161. Song, S., et al., *Serum cystatin C in mouse models: a reliable and precise marker for renal function and superior to serum creatinine.* Nephrol Dial Transplant, 2009. **24**(4): p. 1157-61.
162. de Vries, A.P. and T.J. Rabelink, *A possible role of cystatin C in adipose tissue homeostasis may impact kidney function estimation in metabolic syndrome.* Nephrol Dial Transplant, 2013. **28**(7): p. 1628-30.
163. Wiedemann, M.S., et al., *Short-term HFD does not alter lipolytic function of adipocytes.* Adipocyte, 2014. **3**(2): p. 115-20.
164. Cipriani, S., et al., *FXR activation reverses insulin resistance and lipid abnormalities and protects against liver steatosis in Zucker (fa/fa) obese rats.* J Lipid Res, 2010. **51**(4): p. 771-84.
165. Porez, G., et al., *Bile acid receptors as targets for the treatment of dyslipidemia and cardiovascular disease.* J Lipid Res, 2012. **53**(9): p. 1723-37.
166. Solomon, T.P., et al., *Progressive hyperglycemia across the glucose tolerance continuum in older obese adults is related to skeletal muscle capillarization and nitric oxide bioavailability.* J Clin Endocrinol Metab, 2011. **96**(5): p. 1377-84.
167. Flisinski, M., et al., *Influence of different stages of experimental chronic kidney disease on rats locomotor and postural skeletal muscles microcirculation.* Ren Fail, 2008. **30**(4): p. 443-51.
168. Flisinski, M., et al., *Decreased hypoxia-inducible factor-1alpha in gastrocnemius muscle in rats with chronic kidney disease.* Kidney Blood Press Res, 2012. **35**(6): p. 608-18.
169. Olivares-Reyes, J.A., A. Arellano-Plancarte, and J.R. Castillo-Hernandez, *Angiotensin II and the development of insulin resistance: implications for diabetes.* Mol Cell Endocrinol, 2009. **302**(2): p. 128-39.
170. Chujo, D., et al., *Telmisartan treatment decreases visceral fat accumulation and improves serum levels of adiponectin and vascular inflammation markers in Japanese hypertensive patients.* Hypertens Res, 2007. **30**(12): p. 1205-10.

6 Curriculum Vitae

Publications

1. **Chin S**, Item F, Wueest S, Zhou Z, Wiedemann M, Gai Z, Schoenle E, Kullacl-Ublick G, Al-Hasani H, Konrad D. *Opposing effects of reduced kidney mass on liver and skeletal muscel insulin sensitivity in obese mice.* Diabetes, 2014 (DB_140779.R1, sumitted 15-May-2014 and published 16-Oct-2014)

2. Gai Z, Hiller C, **Chin SH**, Hofstetter L, Stieger B, Konrad D, Kullal-Ublick GA. *Uninephrectomy augments the effects of high fat diet induced obesity on gene expression in mouse kidney.* Biochim Biophys Acta, 2014.

3. Wueest S, Mueller R, Blüher M, Item F**, Chin AS**, Wiedemann MS, Takizawa H, Kovtonyuk L, Chervonsky AV, Schoenle EJ, Manz MG, Konrad D. *Fas (CD95) expression in myeloid cells promotes obesity-induced muscle insulin resistance.* EMBO Mol Med, 2014. **6**(1): p. 43-56.